MASTER OF SCIENCE THESIS

COMPOUNDING AND CHARACTERIZATION OF TIRE TREAD COMPOUNDS USING FUNCTIONALIZED RUBBER

SIMON REZELMAN

S1721542

MSC. MECHANICAL ENGINEERING

DEFENSE DATE: 19-07-2023

PLACE: HORST HR N109

UNIVERSITY OF TWENTE.

COLOPHON

MANAGEMENT
Elastomer Technology and Engineering (ETE), Department of Mechanics of Solids, Surfaces and Systems (MS3), Faculty of Engineering Technology

DATE
Starting date: July 1st 2022
Defense date: July 19th 2023

PROJECT
Compounding and characterization of tire tread compounds using functionalized rubber

AUTHOR
Simon Rezelman
s1721542
MSc. Mechanical Engineering

GRADUATION COMMITTEE
Prof.Dr. A. Blume (Chair)
ET-ETE
Dr. F. Grunert (Supervisor)
ET-ETE
Dr.Ir. W.J.B. Grouve (External)
ET-PT

POSTAL ADDRESS
P.O. Box 217
7500 AE Enschede

WEBSITE
www.utwente.nl

PREFACE

Tires are one the most commonly used rubber products in the world and have been used for a very long time. Still, improvements can be made with regards to longevity, safety and efficiency. Rubber technology had already piqued my interest when following courses for my master's degree, and the ambition grew to gain more experience in this field. I took the opportunity to perform my graduation project in the research chair Elastomer Technology and Engineering, investigating the effects of using functionalized elastomers, as well as high and low surface area silica in tire tread compounds, taking into account their production process, as well as final material properties. The project resulted in more insight into the effectiveness of rubber functionalization, showing that the "Magic Triangle" of tire design can be extended further.

I want to thank my supervisors prof. dr. Anke Blume and dr. Fabian Grunert for their heaps of collective knowledge and their guidance during this project. I really value your effort within my graduation project, but also your interest in my future career. I also want to show my appreciation to ir. Anmol Aggarwal. You taught me a lot in the first months, teaching me all aspects of rubber production and testing, and were always available to discuss any questions I had throughout the whole graduation project. Last but not least, I would like to express my gratitude to my girlfriend and my family. Your unconditional support through these years means a lot to me.

TABLE OF CONTENTS

ABSTRACT

Recent EU regulations to reduce CO_2 emissions from passenger cars have driven automotive manufacturers to research new materials and technologies to make their vehicles more efficient. One of these aspects is reducing rolling resistance of the tires, which makes vehicles more fuel efficient. This reduction in rolling resistance must be achieved while also maintaining or improving tire safety and longevity. Rolling resistance has already been reduced significantly with the introduction of the “Green Tire”, a tire tread consisting of synthetic elastomer blends combined with a silica/silane filler system. Improvements can still be made by modifying the elastomer with functionalized groups, which can improve the interaction between the silica filler material and the elastomer.

In this research, model tire tread compounds were produced using a variety of functionalized and non-functionalized elastomers, combined with varying silica filler types and contents. Multiple aspects of these compounds were characterized, such as their processibility, curing behavior and their (dynamic) mechanical properties.

Based on these results, it was concluded that functionalization of an elastomer has an impact on almost every aspect of tire tread design, with the processability of the compound being negatively affected by a filler-elastomer interaction that occurs before curing of the compound, increasing its viscosity. However, the usage of a functionalized rubber in a model tire tread compound results in a reduction in the rolling resistance indicator tan(δ), while not having any significant effects on the mechanical properties.

CHAPTER 1
INTRODUCTION

1.1 General information

Due to an increase in the use of road transport, the emission of greenhouse gases in the European Union by this sector has increased by more than 30% from 1990 to 2019. Over 70% of these emissions are caused by light trucks and passenger cars [1]. As a response, the EU has adopted regulations that target the reduction in CO_2 emissions. New passenger cars and vans from 2030 to 2034 should reduce emissions by 55% and 50% respectively, and the new vehicles sold from 2035 should reduce their emissions by 100% as compared to their 2021 levels [2].

Automobile manufacturers are pushed to find solutions to reduce these emissions by making vehicles more aerodynamic, their engines more efficient, and finding alternative propulsion methods. Another way of reducing emissions is by reducing the rolling resistance of the tires. A reduction in rolling resistance decreases the amount of power consumed to keep a car at speed, saving fuel consumed by the internal combustion engine, and therefore reducing emissions by the vehicle. Additionally, heat build-up in the tire is reduced, as the hysteretic losses causing rolling resistance are transferred into heat. With the transition towards Electric Vehicles (EV's), reduction of the energy consumption of the vehicle stays relevant, as the rolling resistance has a significant impact on the range of an EV [3].

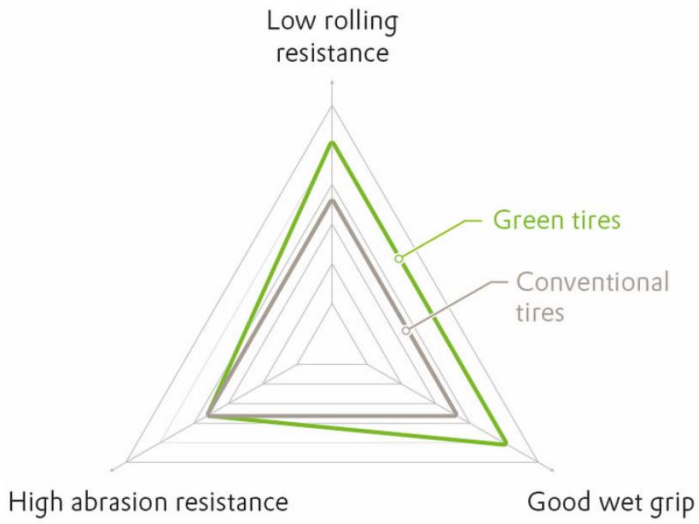

Figure 1: The "Magic Triangle" tradeoff between abrasion resistance, rolling resistance and wet grip [4].

The main influence on the rolling resistance of a tire is the design of the tire tread. Early tire treads used emulsion styrene-butadiene rubber and carbon black as a filler. Using this combination of materials, a balance has to be found between rolling resistance, wear resistance, and grip, with improvement in one aspect always negatively affecting the other properties. The "Green Tire" was developed in the early 1990's, introducing an elastomer blend of styrene-butadiene and butadiene, as well as a silica/silane filler system. Rolling resistance and wet grip were considerably improved while not affecting the wear resistance of the tire tread significantly, shown visually in Figure 1 [4].

Currently, the use of rubber functionalization to improve tire properties is investigated. There are some commercial grades of functionalized styrene-butadiene rubber available. The intended goal of this rubber functionalization is to improve the interaction between the rubber and the filler, specifically the silica filler that is used in modern passenger car tires [5].

1.2 Aim of the project

The main goal of this project is to determine the influence of using functionalized styrene-butadiene rubbers in a tire tread compound on the processability, mechanical properties, and the dynamical properties of the compound.

Secondary goals are to investigate the effects of using an elastomer blend in combination with varying silica specific surface areas, as well as silica content.

1.3 Thesis outlay

In this research, the effect of functionalization of styrene-butadiene rubber on the processability, mechanical properties, and tire performance indicators is investigated. This is done by comparing two different types of functionalized styrene-butadiene rubbers in the context of a modern tire tread compound. This includes the use of an elastomer blend with both styrene-butadiene rubber and butadiene rubber. Three types of highly dispersible silica with differing specific surface area are used in these compounds in various loadings.

To analyze the processability of the compounds, their mixing procedure is recorded. In addition, curing characteristics, Mooney viscosity, and Payne effect measurements are analyzed for all compounds. Mechanical and dynamic properties are also investigated, including tensile, hardness, and rebound tests. Selected samples are subjected to dynamic mechanical analysis, and their loss angle and glass transition temperature are recorded.

CHAPTER 2
LITERATURE SURVEY

2.1 History of rubber

The earliest recorded use of rubber products dates back to the late 15th century when Christopher Columbus explored South America. It was seen that South American Indians used sap extracted from trees to produce balls for ceremonial games. This sap was also used for waterproofing of clothes, footwear, and bottles. It took until the early 18th century for renewed interest in rubbers by the western world. During this time the terms “rubber” and “caoutchouc” were coined and more and more applications were invented. Natural Rubber (NR) became more widely used and demand increased. Usually, NR was transported in dried clumps and subsequently cut up or dissolved to make products. With the invention of the masticator by John Hancock, rubber was more easily processed. Multiple pieces of rubber could be masticated and mixed into a single, consistent mass, aiding the further processability of the product [6].

Improvement in the mechanical properties was achieved with the invention of the vulcanization process by Charles Goodyear in 1839. In this process, sulfur (in combination with accelerators) is added to a rubber compound and cured at an elevated temperature. Vulcanization of rubber improves the tensile properties, while making it more resistant to wear and swelling. The properties also become more consistent over a great temperature range. With these improved properties, NR became a suitable material for use in tires [7].

With the explosion of popularity of the bicycle and later the automobile towards the end of the 19th and start of the 20th century, the demand for NR grew rapidly. The latex for the production of natural rubber is extracted by “tapping” the Hevea Brasiliensis trees. In earlier times, this was done using wild trees, scattered in the Brazilian jungle. In an effort to better organize the cultivation of the rubber trees, seeds of the Hevea Brasiliensis were shipped to Sri Lanka and Singapore around 1876. The production of NR was made more efficient by organizing the cultivation of rubber trees in large plantations. This increased the production from ~ 100,000 metric tons in 1909 to over 14 million metric tons in 2021. Asian rubber production overtook South American rubber production in less than 30 years [6], [8], [9].

In an effort to satisfy the increasing demand of NR, attempts to make a synthetic version are reported as early as 1906. One of the first successful synthetic rubbers is Butadiene Rubber (BR), which used a butadiene monomer and a sodium catalyst. Butadiene rubber is still used to this day, however the production process has been improved and catalysts have changed to improve the material properties and production speed. Butadiene rubber has become increasingly popular for use in tire treads of passenger cars, as it has superior rolling resistance and wear properties in comparison to natural rubber. In addition to butadiene rubber, styrene and butadiene were also co-polymerized to create Styrene-Butadiene Rubber (SBR). SBR has similar advantages over NR, making it suitable for use in tire treads as well [10].

2.2 Rubbers used in tire treads

2.2.1 Natural rubber

Natural rubber consists of mainly cis-1,4 polyisoprene units (Figure 2), with high molecular weight. Due to its high cis content, NR has a low glass transition temperature. Strain-induced crystallization also occurs in the rubber. This makes natural rubber a material with a high tensile strength, wear resistance, and tear resistance. These properties make NR still suitable for use in tires today. Offroad tires use up to 45% (of tire weight) of NR, as durability is very important in this application. Natural rubber compounds show low oil resistance and aging properties. In addition to that, wet grip and traction properties are relatively poor. This is why tires for use on passenger cars use less NR, as (wet) grip is very important for safety at high speeds. In this case, NR in the tire tread is substituted by synthetic alternatives [11], [12].

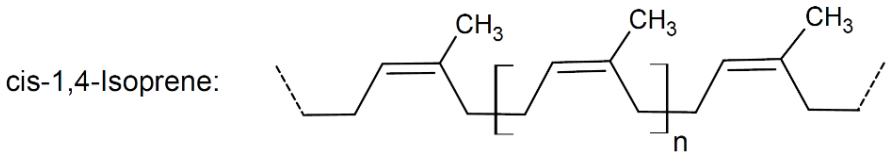

Figure 2: Natural rubber chemical structure [13].

2.2.2 Butadiene rubber

Butadiene Rubber (BR) consists of butadiene monomers, polymerized by a variety of catalysts. Unlike NR, butadiene polymerizes in a variety of orientations, as shown in Figure 3. Depending on the catalyst, the content of cis, trans, and (iso- and syndiotactic) vinyl, as well as the branching structure can be influenced. This in turn affects the glass-transition temperature and other properties of the rubber. A high cis content improves the abrasion resistance, elasticity, fatigue life, and tear strength of the rubber, as its linear nature promotes strain-induced crystallization and a low glass transition temperature.

Being non-linear, a vinyl group inhibits the free rotation of the polymer chain. Therefore the glass transition temperature increases with higher vinyl content, showing high viscoelastic energy dissipation. This also improves fatigue life, but less significantly than high cis BR. High cis BR, typically with a cis-content above 90%, is therefore usually desired in tire treads. One of the drawbacks of using BR is the poor wet grip properties. To improve the wet grip properties when used in a tire tread, BR is commonly blended with styrene-butadiene rubber [11], [14], [15].

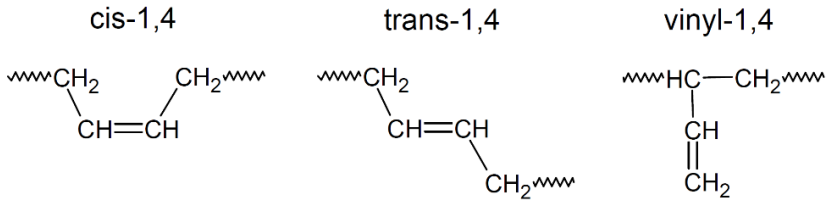

Figure 3: Possible polybutadiene chemical structures [14].

2.2.3 Styrene-butadiene rubber

Butadiene can be polymerized in combination with styrene, creating Styrene-Butadiene Rubber (SBR). The butadiene part of the rubber can have the same structures as seen in Section 2.2.2 Butadiene rubber, with the addition of a styrene group. This adds a variety of configurations as shown in Figure 4, affecting the properties of the material. Polymerization can be done using an emulsion or a solution process, resulting in emulsion-SBR (E-SBR) and solution-SBR (S-SBR).

Production of E-SBR is relatively cheap, and is therefore preferred when using SBR in conventional passenger car tires. However, the only parameters that can be adjusted when producing the material are the molecular weight and the styrene/butadiene ratio. This limits the degree of adjustment available to the structure and therefore the properties of the material. As a result, the produced material has a random ratios of cis, trans, and vinyl. In addition to the lack of adjustment in the production process, a lot of emulsifying agents and processing aids remain in the final product, which is undesirable in the context of tire tread application. These remaining additives affect multiple final properties, such as the curing speed and decreased modulus of the final product [11], [16].

In contrast to E-SBR, the production of S-SBR is more expensive. However, the production process is more controllable, resulting in more control over the microstructure of the butadiene part and the ability to create a more linear polymer chain with less branching. This mainly improves the elasticity, as well as rolling resistance and wet grip indicators of the material. Also, almost all solvents are extracted from the material after polymerization, resulting in a much more pure product. The mechanical properties of S-SBR suffer slightly compared to E-SBR, as it is more difficult to produce S-SBR with a higher molecular weight [11], [15], [16].

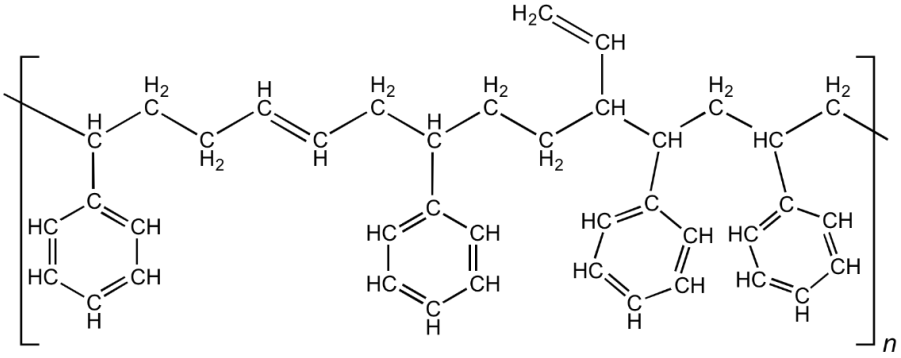

Figure 4: A selection of possible orientations and structures of styrene-butadiene rubber [17].

2.2.4 Functionalized styrene-butadiene rubber

To improve the properties of SBR even further, functional groups can be added to the polymer. These functional groups are designed to improve interaction with filler materials mainly through covalent or hydrogen bonding between polymer and filler. Rubber functionalization can be achieved through several methods, as can be seen in Figure 5. In solution polymerization, the chain end can be terminated with the use of a functionalized agent. This results in a chain-end functionalized polymer. Some initiators used in solution polymerization can also be modified to have a functional group, resulting in a polymer with initiator functionalization. Another technique is to add functionalized monomers to the mix of styrene and butadiene. In this process, the functionalized monomer copolymerizes

together with styrene and butadiene, resulting in the possibility of multiple functionalized groups in the backbone of the polymer chain. Lastly, the double bonds in the vinyl groups can be modified after polymerization of the rubber, resulting in functionalization in side chains that were previously vinyl groups [15], [18], [19].

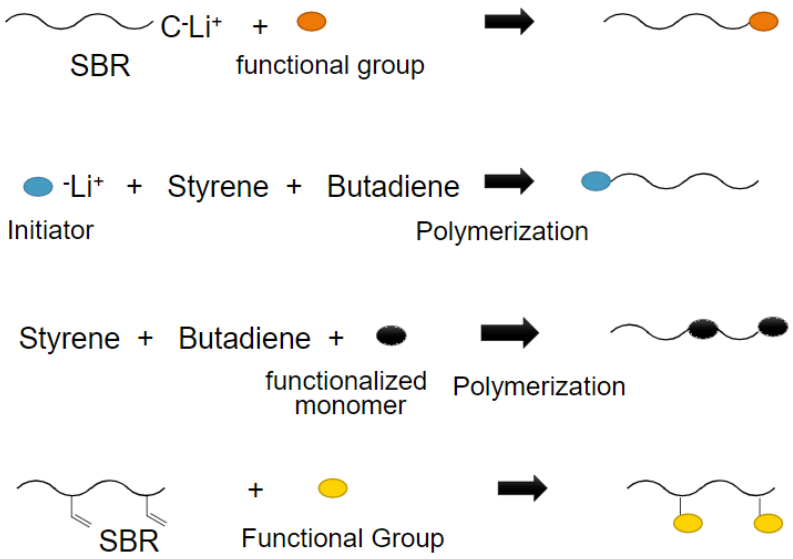

Figure 5: Different methods of polymer functionalization [18].

SBR for use in tire tread compounds is typically functionalized with polar groups. This improves the affinity with the polar silica filler. Through this functionalization, the filler dispersion improves, resulting in less large clusters of silica. This in itself makes the filler more effective in improving the properties of the compound. Additionally, the improved interaction between the filler and the functionalized polymer results in improved hysteresis properties at high temperatures, while also increasing wet grip [20]–[22].

One of the main drawbacks of polymer functionalization is the addition of the functionalized structures themselves. To some degree in initiator- and end- functionalization, but especially in the case of backbone and side chain functionalization, the addition of a bulky functionalized group deteriorates chain mobility. This results in a significant viscosity increase compared to non-functionalized rubbers, resulting in worse processability of the compound [15].

2.3 Rubber reinforcement

Fillers are used in rubbers to improve the mechanical properties of the end product. Typically, the addition of fillers to polymeric materials increases the modulus and hardness of the material, but deteriorates the elongation at break. For elastomers however, certain fillers can improve the tensile strength and modulus, while also improving the maximum elongation. These materials are known as reinforcing fillers. The most common reinforcing fillers used in rubber are carbon black and silica [23], [24].

2.3.1 Carbon black

Carbon black filler consists of carbon particles of very specific shape and size. Carbon black is commonly produced using the furnace black process. In this process, aromatic oils are injected into a stream of hot gas, where the oil pyrolyzes, forming carbon black aggregates. Several parameters in this process can be adjusted so that the carbon black aggregates have a specific size and structure [25], [26]. The size and structure of the carbon black is important, as they have a major influence on the reinforcement of the rubber product. With increasing surface area (smaller particles), more area of the carbon black particles is able to interact with the polymer chains of the elastomer, therefore having a larger reinforcement effect. This comes with the disadvantage of increased compound viscosity and deteriorated filler dispersibility [24], [26]. In tire treads, the use of carbon black as a reinforcing is very common. However, a tradeoff always has to be made between wear resistance and hysteresis performance when adjusting the structure and surface area of the filler [4].

2.3.2 Silica/silane

To improve the tradeoff between hysteresis and wear resistance, a silica filler system is commonly used in tire tread compounds. Silica is most commonly produced using precipitation, where a sodium silicate solution and an acid react in a vessel. This reaction results in silica precipitating and suspending in water. After filtration and drying, a silica powder is obtained, that can be processed and used in rubber products. As with carbon black, processing parameters can be adjusted to obtain silica particles with specific size and structure, resulting in products with different reinforcement potential [27].

Silica by itself is not suitable for use in the tire tread, as polar silanol groups are present on the surface of silica particles. Typical rubbers in tire applications are non-polar. To improve compatibility between the elastomer and silica, coupling agents such as silanes are used. A silane is added during mixing, and an optimum temperature range is requited for the silanization reaction to occur. This is a reaction where the silane forms covalent bonds with the silica while releasing alcohols, and can be seen in Figure 6.

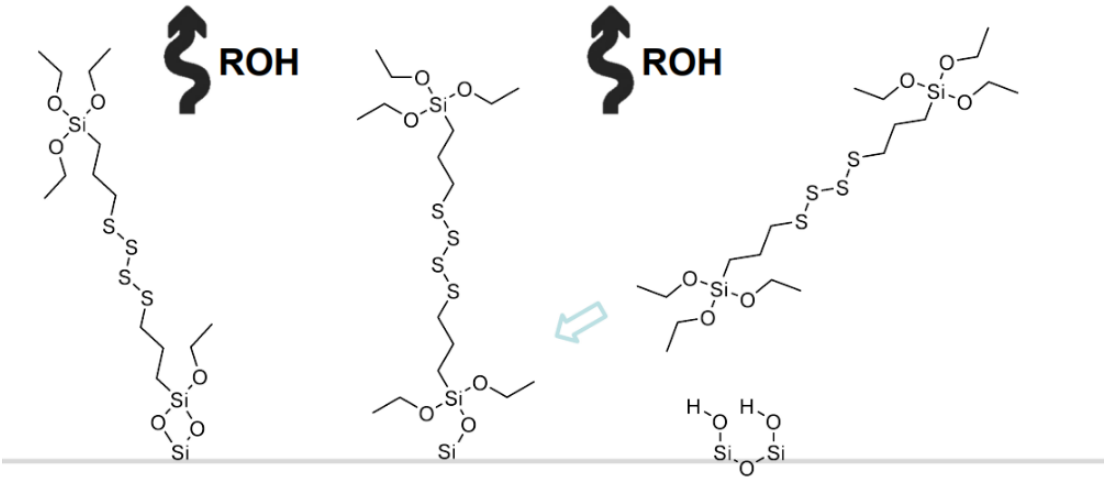

Figure 6: Silanization reaction, primary reaction [28].

Additionally, a secondary condensation reaction can occur where silane molecules couple to each other, shielding silanol groups on the silica surface from their surroundings. This decreases the polarity of the silica, improving the dispersion of the filler in the rubber compound, shown in Figure 7.

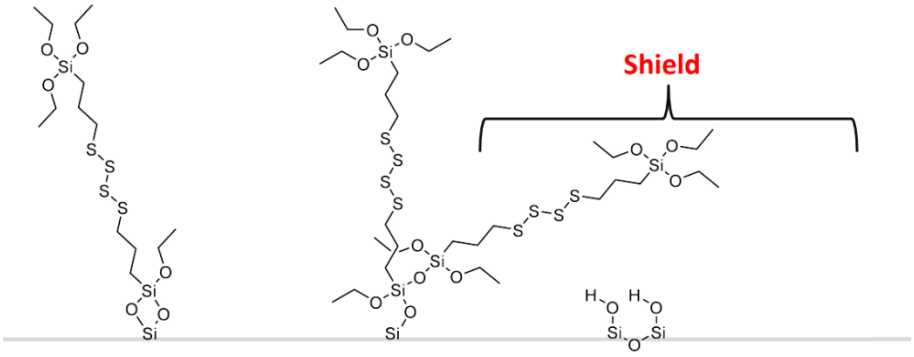

Figure 7: Silanization reaction, secondary reaction[28].

Subsequently, when the rubber is cured, the silica can crosslink with the polymer chain for a strong interaction between rubber and silica, as is schematically shown in Figure 8 [11], [28], [29].

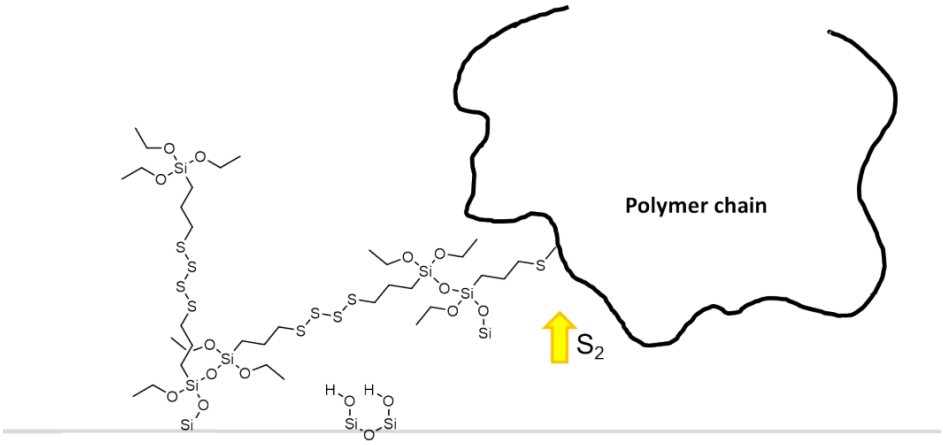

Figure 8: Silica-polymer coupling [28].

The result of silica-silane-rubber coupling in a rubber compound is an increased reinforcement of the rubber compared to other systems such as rubbers with carbon black. This increase in reinforcement improves tear and wear resistance over compounds that do not use silane. The silica/silane system increases the modulus of a compound compared to a carbon black filler system with the same surface area and structure. Additionally, hysteresis properties improve with the usage of a silica/silane reinforcement system, changing the dynamic response in relation with temperature [11], [20], [30]. In application of a tire tread, a similar wear resistance to a tread using carbon black is achieved, while increasing the wet grip properties, decreasing rolling resistance, and decreasing heat buildup.

2.4 Viscoelasticity of rubber

Rubbers show the unique property of viscoelasticity. This is a combination of elasticity and viscosity. A material is considered elastic if it deforms as a force is exerted onto that solid and returns to its original shape after the force is removed. Viscosity is the internal friction that arises when a material is deformed [31], [32].

Using Dynamic-Mechanical Analysis (DMA), the viscoelastic behavior of rubbers can be investigated. In DMA, a rubber sample is subjected to prescribed sinusoidal strain loading, where stress is recorded. In purely elastic materials, the stress and strain should be in phase, i.e. the stress and strain reach a peak at the same time. For purely viscous materials, the stress lags behind the strain 90 degrees (phase lag). Viscoelastic materials have a phase lag somewhere in between. The recorded stress response can be divided into two components: the in-phase elastic stress component (Storage modulus, G' or E') and the phase-delayed viscous stress component (Loss modulus, G'' or E''). From the ratio E''/E', the loss angle (tan(δ)) is calculated, which gives an indication of what amount of energy is lost during deformation [20], [31].

Damping properties of elastomers are temperature dependent, so typically tan(δ) is measured over a temperature range between -80 °C and 80 °C, with a resulting graph shown in Figure 9. Using this curve, laboratory indicators of several tire performance properties can be obtained, such as wet grip, rolling resistance, and wear resistance [20], [31]. Additionally, the glass transition temperature (T_g) can be determined using DMA, as the peak of the curve approximates the glass transition of the material. This measurement is frequency dependent, with the measured T_g increasing with increasing cyclic frequency [33]. However, it allows for compounds to be compared among themselves, if the same cyclic frequency is maintained.

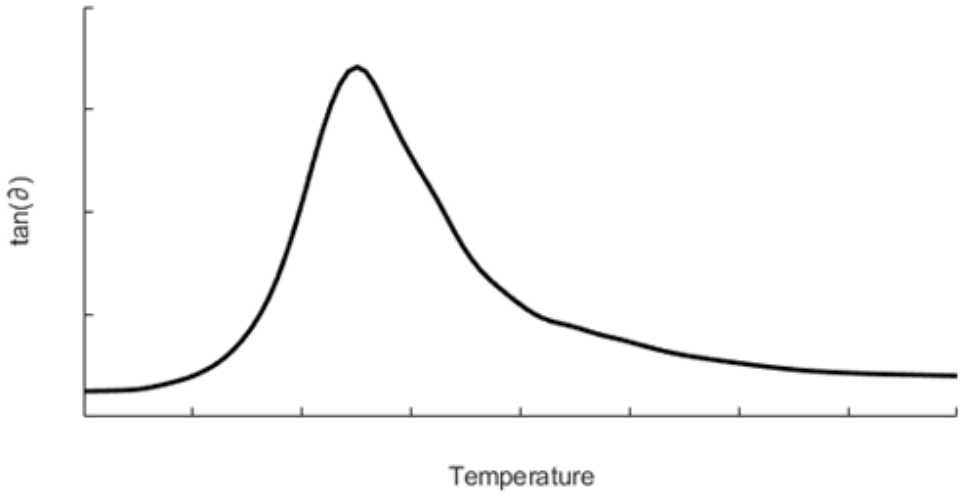

Figure 9: Tangent delta - temperature dependency [34].

2.5 Tire performance

Tire labelling has been mandatory in the EU in some form since 2012, with the newest legislation introduced in 2021. These tire labels, shown in Figure 10, show classifications for rolling resistance, wet grip, and noise. More recent additions are grip performance in severe snow conditions or in extreme climatic situations [35].

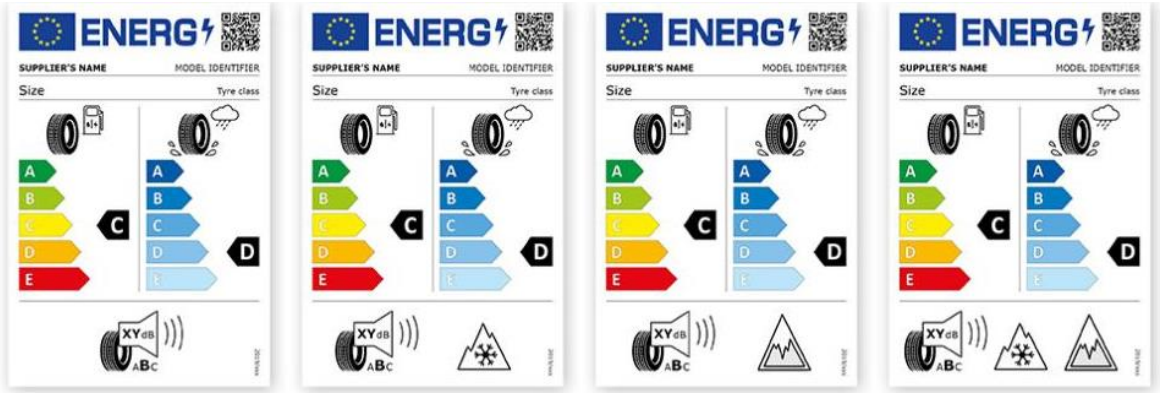

Figure 10: Standard European tire labels [35].

2.5.1 Tire noise

Tire noise is generated due to the tire tread interacting with the road surface at high frequency. [36], [37]. Several mechanisms are at play here, but one of the main contributors to tire noise in consumer tires is the air pumping mechanism. With this mechanism, air is captured in the tire tread and porous cavities in the road surface as the tire rolls over. As the contact patch of the tire deforms during rolling, the air that is captured is pressurized and escapes as the contact is released. This sound generation mechanism is strongly depending on the tire tread pattern, road surface of the road, and driving speed of the vehicle [36], [38].

2.5.2 Rolling resistance

Rolling resistance is the energy loss by rolling the tire over the road surface. Due to the load of the vehicle being exerted on the tires, both the sidewall and tread of the tires are deformed, resulting in energy losses from hysteresis. Typically, this is the second highest contributor to fuel consumption in vehicles using internal combustion engines, with drivetrain losses being the highest contributor [20]. Rolling resistance lab indicators of the tire tread can be investigated using dynamic mechanical analysis, with the loss angle at high temperatures being used for comparison between tire tread compounds [11], [20], [24].

2.5.3 Wet grip

Traction in wet conditions is dependent on both the tread compound and the tread pattern, with the latter mainly being responsible for the evacuation of water between the tread and road surface, preventing aquaplaning . Wet traction can be investigated by using DMA, with the loss angle at 0 °C being used for comparison between compounds [11], [24].

2.5.4 Wear resistance

Wear resistance is not mentioned on the mandatory tire label. However, it is a very important property when producing a tire tread and a standard tread wear rating is always marked on a tire sidewall. A long-lasting tire is much more desirable, both in the economic and environmental sense. A longer lasting tire gives a better return on investment while also releasing less wear particles into the environment. One important indicator is the glass transition temperature (T_g) of the rubber compound used in the tire tread. A linear relation between the T_g and the wear resistance of a rubber exists, with the wear resistance decreasing with increasing T_g [11].

CHAPTER 3
EXPERIMENTAL

3.1 Materials

3.1.1 Elastomers

In this research, two types of S-SBRs and two types of BRs were used. The SBR types used were Sprintan® SLR 4601 and Sprintan® SLR 4602 (Synthos S.A), in the rest of this report referred to as SBR 4601 and SBR 4602, respectively. The BR types used in this research were Buna® Cis-132 (Synthos SA) and Buna® CB-24 (Arlanxeo SA), in the rest of this report referred to as BR Cis-132 and BR CB-24, respectively. Both SBRs were end-functionalized, however SBR 4601 is known to only interact with carbon black, where SBR 4602 has functionality for silica. Both BR types have no functionalization. Table 1 shows characteristics of the elastomers. SBR 4601 and 4602 are very similar elastomers with regards to styrene and vinyl content, with the differentiating factors being their type of functionalization and Mooney viscosity.

Table 1: SBR and BR characteristics [39]–[42].

Elastomer	SBR 4601	SBR 4602	BR Cis-132	BR CB-24
Functionalization	Carbon Black	Silica	None	None
Initiator/catalyst	Li	Li	Ni	Nd
Styrene cont. (%)	21.0	21.1	0	0
Vinyl cont. (%)	62.2	62.1	n.a.	n.a.
Cis 1,4 cont. (%)	n.a.	n.a.	95	96
Trans 1,4 cont. (%)	n.a.	n.a.	n.a.	n.a.
Tg (°C)	-25.0	-25.0	-105	-109
Mooney viscosity (MU)	49	63	45	44

3.1.2 Silica

In increasing order of specific surface area (SSA) the following types of high dispersible silica were used: Zeosil 1115MP (Solvay NV), Ultrasil 7000GR, and Ultrasil 9100GR (Evonik Industries AG). One differentiating characteristic (other than varying SSA) is the dosage form of these silica grades. The 1115MP grade has a micropearl structure, while both U7000 and U9100 are granulated. These different dosage forms are to improve dispersibility of the silica in the rubber compound, as untreated silica powder is relatively hard to incorporate. Although both dosage forms improve dispersibility compared to powdered silica, the dispersion mechanisms are different [43]. Table 2 shows the relevant characteristics of the different types of silica used in this research.

Table 2: Silica characteristics [44]–[46].

Silica type	Zeosil 1115MP	Ultrasil 7000GR	Ultrasil 9100GR
Dosage form	Micropearl	Granule	Granule
SSA BET (m2/g)	115	175	235
SSA CTAB (m2/g)	115	160	200

3.1.3 Compound formulation

The formulation of the compounds used in this research were based on a “Green Tire Formulation” [4], [43], meaning that a silica/silane filler system was used for improved rolling resistance and wet traction. The compounds in this research either used pure SBR as 100 phr (parts per hundred rubber), or were blended with BR in 80/20 or 60/40 ratios. Silica loadings and grades were varied, so the amount of silane was adjusted accordingly. The amount of TESPD added to the compound is 0.0725 parts per hundred silica when using the silica grade U7000GR. To account for the varying SSA of the other silica grades, the amount was adjusted according to their respective CTAB number [47]. Plasticizer was adjusted according to 0.3125 parts per hundred silica . When using different silica grades, the relative amount of plasticizer used remained constant, disregarding the SSA of the silica used. A general overview of the compound formulations is shown in Table 3.

Table 3: Tire tread compound formulations.

Series		S1		S2			S3		S4	
Type	Material	phr	phr	phr	phr	phr	phr	phr	phr	phr
Stage 1										
Rubber	SBR 4601	100	-	80	-	-	-	-	80	-
	SBR 4602	-	100	-	80	80	60	60	-	80
	BR Cis-132	-	-	20	20	-	40	-	20	20
	BR CB-24	-	-	-	-	20	-	40	-	-
Filler	Z1115 MP	-	-	-	-	-	-	-	var	var
	U7000 GR	var	var	var	var	var	var	var	-	-
	U9100 GR	-	-	-	-	-	-	-	var	var
	Si 266	var	var	var	var	var	var	var	var	var
	N330	3	3	3	3	3	3	3	3	3
Activator	Stearic acid	2	2	2	2	2	2	2	2	2
	Zinc oxide	2	2	2	2	2	2	2	2	2
Antioxidant	Dusantox 6PPD	2	2	2	2	2	2	2	2	2
Antiozonant	Wax Antilux 654	2	2	2	2	2	2	2	2	2
Plasticizer	Vivatech 500	var	var	var	var	var	var	var	var	var
Stage 2										
Accelerator	Ekaland DPG	1.5	1.5	1.5	1.5	1.5	1.5	1.5	1.5	1.5
Stage 3										
Accelerator	TBBS	1.5	1.5	1.5	1.5	1.5	1.5	1.5	1.5	1.5
	TBzTD	0.4	0.4	0.4	0.4	0.4	0.4	0.4	0.4	0.4
Curative	Sulfur	1.4	1.4	1.4	1.4	1.4	1.4	1.4	1.4	1.4

This research was divided in four compound series, all with different blend ratios, silica types, and silica loadings. Further details about blend ratios, silica type, and silica loadings are given in Table 4. In the first series, the two pure SBR grades were compared. In the second series, two BR types were blended with SBR in an 80/20 ratio. In the third series, the blend ratio between SBR and BR was varied. The fourth series investigated silicas with varying surface areas.

Table 4: Compound series clarification.

Series #	Elastomer(s)	Blend ratio	Silica type	Silica loadings	# of compounds
1	4601/Cis-132	100/0	U7000GR	30/60/90	6
	4602/Cis-132	100/0	U7000GR	30/60/90	
2	4601/Cis-132	80/20	U7000GR	0/30/60/75/90	15
	4602/Cis-132	80/20	U7000GR	0/30/60/75/90	
	4602/CB-24	80/20	U7000GR	0/30/60/75/90	
3	4602/Cis-132	60/40	U7000GR	0/30/60/75/90	10
	4602/CB-24	60/40	U7000GR	0/30/60/75/90	
4	4601/Cis-132	80/20	U9100GR	30/60/90	12
	4602/Cis-132	80/20	U9100GR	30/60/90	
	4601/Cis-132	80/20	Z1115MP	30/60/90	
	4602/Cis-132	80/20	Z1115MP	30/60/90	

3.2 Compounding and curing

3.2.1 Mixing

Mixing was done in a three-stage mixing regime using a Brabender Plastograph 350S internal mixer, after which the compounds were sheeted out using a Polymix 80T two-roll mill. Between all mixing steps, the compounds were stored for at least 16 hours to allow the polymer chains to relax. All produced compounds in this research followed the same procedure which is shown in Table 5.

In the first stage, the polymer(s), reinforcement system, plasticizer, activator, and protective additives were mixed. A fill factor of 72% was used, with a starting temperature and speed of 80 °C and 70 rpm respectively. Filler was added in two steps, with the first step containing 1/2 or 2/3 of the silica/silane dosage and the second step containing 1/2 or 1/3 of the silica/silane dosage, plasticizer, activator, and protective agents. The addition of filler in two steps was done to prevent the mixer from exceeding its torque limitations. At high filler loadings (≥ 60 phr) the volume of elastomer is relatively low compared to the filler volume. This means that 2/3 of the filler can be added in the first step. Due to the elastomer volume being relatively high at low filler loadings (< 60 phr), the amount of filler added in the first step was reduced. Isothermal mixing was performed at a temperature of 140 °C to promote silanization. Due to differences in torque due to variation in filler loading and SSA, the required temperature for silanization may be reached at different times, and therefore silanization times are different. However, as the leading influence on the degree of silanization is temperature, silanization time is of less importance [48] Therefore, the mixing time remained constant.

In the second stage, further silanization and filler dispersion are promoted. Furthermore, N,N'-Diphenyl Guanidine (DPG) was added to function as an accelerator and silanization catalyst [49]. Additionally, DPG is absorbed by the silica surface as a secondary accelerator, preventing the primary accelerators added in the next stage from being absorbed, preventing a long time to scorch and slow cure rate. The fill factor of the internal mixer was reduced to 69% to account for any losses in the compound. The starting temperature remained at 80 °C, while the initial rotor speed was increased to 80 rpm to reach the silanization temperature quicker.

The vulcanization system, consisting of Sulphur, TBBS, and TBzTD was added in the third stage. Again, the fill factor was reduced to 66% to account for any losses. To prevent pre-scorch, the initial temperature and speed of the mixer were reduced to 50 °C and 50 rpm respectively.

Table 5: Mixing regime.

Stage 1	
Fill factor (%):	72
Initial temperature (°C):	80
Initial rotor speed (rpm):	70
Time (m:ss)	Step
-0:30	Add raw rubber
0:00	Ram down, start measurement
1:00	Ram up, add 1/2 or 2/3 of silica & silane
1:30	Ram down
2:30	Ram up, add oil, chemicals, and 1/2 or 1/3 of silica & silane
3:00	Ram down
4:00	Ram up, sweep hopper and ram
4:15	Ram down, isothermal mixing at 140 °C
7:00	Dump, check weight and dump temperature
	Sheet out 5x on two-roll mill
Stage 2	
Fill factor (%):	69
Initial temperature (°C):	80
Initial rotor speed (rpm):	80
Time (m:ss)	Step
0:00	Add batch stage 1, ram down, start measurement
0:50	Ram up, add DPG
1:00	Ram down, isothermal mixing at 140 °C
5:00	Dump, check weight and dump temperature
	Sheet out 5x on two-roll mill
Stage 3	
Fill factor (%):	66
Initial temperature (°C):	50
Initial rotor speed (rpm):	50
Time (m:ss)	Step
0:00	Add batch stage 2, ram down, start measurement
0:30	Ram up, add vulcanization system
3:00	Dump, check weight and dump temperature
	Sheet out 5x on two roll mill

3.2.2 Vulcanization

Vulcanization of the produced compounds was performed using a Wickert WLP 1600 press. This press was used to produce compression molded sheets and cylinders. A ~2 mm thick square mold was used for the tensile sheets. The cylinders were produced using a mold with a thickness of 12 mm and a diameter of 28 mm. The samples were molded at a pressure of 100 bar and 160 °C. Silica filled compounds show a marching modulus behavior which is influenced by the degree of silanization and flocculation [48]. Excessive flocculation was prevented by performing vulcanization within 16-20 hours after the last mixing step. Due to the variety in silica loadings and SSA, varying intensities of marching modulus were still observed. Therefore, a fixed curing time was set at 30 minutes for a fair comparison of properties for the compounds. The cylinders were cured for an additional 5 minutes to account for the larger thickness of the mold.

3.3 Characterization

3.3.1 Mooney viscosity

Mooney viscosity was measured by a Mooney 2000 Viscometer (Alpha Technologies) and Mooney Premier (Alpha Technologies). Mooney viscosity indicates processability of the compound. An ML(1+4) measurement was performed at 100 °C according to ISO 289 [50]. As there was a transition from one machine to another, some sample tests were repeated to verify the results between both machines.

3.3.2 Payne effect

Payne effect measurements record the shear moduli of the compounds over a strain range. The difference in storage modulus between low and high strain is used as an indicator of filler dispersion. This measurement was done using the Rubber Process Analyzer (RPA) Elite (TA instruments). The measurements were performed at 60 °C and 1.667 Hz from 0.075% to 100% strain in 2 sweeps. The first strain sweep was performed from low to high strain, the second sweep was performed from high to low strain. This was done because silica filled compounds show flocculation, where silica particles form clusters during storage [51]. This manifests in a higher storage modulus at low strain in the first sweep. In the second sweep, the network is broken down, so a lower storage modulus at low strain is seen.

3.3.3 Vulcanization behavior

Vulcanization behavior was measured using a rotorless oscillating shear rheometer, the RPA Elite (TA instruments). According to ISO 6502 [52], the low-strain vulcanization behavior was measured at 0.5° strain, 1.67 Hz and 160 °C. The test was performed for 30 minutes.

3.3.4 Hardness

A Zwick Shore A hardness tester, calibrated with Rex durometer test blocks was used to test the hardness of the cured compounds. This measurement was done according to standard ASTM D2240 [53]. Cylindrical test pieces with a thickness of 12 mm and a diameter of 28 mm were used. Hardness tests were performed on both flat surfaces, after which the average was taken of those two values.

3.3.5 Stress-strain behavior

Tensile tests were performed on a Zwick Z01 (Zwick Roell GmbH) tensile tester according to standard ISO 37 [54], using Type 2 dumbbells cut from a ~2 mm thick sheet. Three dumbbells were used per compound, and the measurements were done with a crosshead speed of 500 mm/min and a pre-tension of 0.1 MPa. The median curve and average of ultimate values is used for later evaluation. The resulting data consisted of a stress-strain graph, average stress and strain at break, moduli at several strains, and reinforcement index.

3.3.6 Rebound resilience

Rebound resilience tests were performed at room temperature on a Zwick 5109 Rebound Resilience Tester (Zwick Roell GmbH) according to ISO 4662 [55]. Cylindrical test pieces with a thickness of 12 mm and a diameter of 28 mm were used. Rebound tests were performed on both flat surfaces, after which the average was taken of those two values.

3.3.7 Dynamic mechanical analysis

Dynamic properties were determined using a Metravib Visco-analyser 2000 DMA (Acoem Metravib). According to standard ISO 4664 [56], a temperature sweep was performed from -80 °C to + 80 °C with an increment of +2 °C per minute. This measurement is performed under constant static and dynamic strain. Static strain, dynamic strain, and dynamic frequency were set to 3%, 1%, and 10 Hz, respectively. A 35 x 5,5 mm sample was cut from a ~2 mm thick sheet and subjected to a tensile load. The resulting data used in this research is a loss angle at specific temperatures.

CHAPTER 4
RESULTS AND DISCUSSION

4.1 Series 1: Pure SBR compounds, varying SBR type

4.1.1 Processability

Mixing curves

During the first stage mixing (Figure 11), compounds using 100% SBR 4602 show a faster temperature rise compared to compounds using SBR 4601. During mastication and right after adding silica in the first mixing stage, required rotor torques are similar. During isothermal mixing, the rotor torque decreases significantly for SBR 4601 compounds, while SBR 4602 compounds show only a slight decrease. The compounds show this behavior regardless of silica content. But, as expected, temperature and end torque rise with increasing silica content. Unfilled SBR 4601 has a lower viscosity than SBR 4602, so a higher torque (and more heat generation) is to be expected when mixing. In the second and third mixing stages, the rotor torque is similar between the two SBR types, but SBR 4602 shows a higher temperature increase.

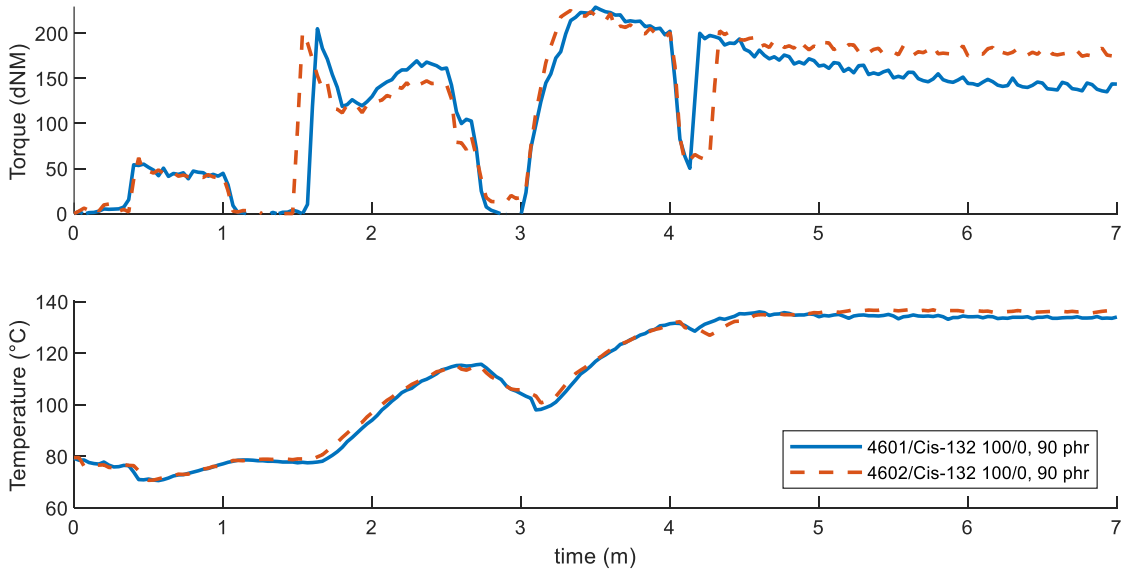

Figure 11: Torque and temperature, 1st mixing stage, pure SBR 4601/4602 using 90 phr silica.

Mooney viscosity

Mooney viscosity of the compounds, as shown in Figure 12, supports the findings in the previous section. With the usage of SBR 4602, the viscosity increases significantly over all filler loadings. Based on Figure 12, an increase of ~30 MU is to be expected when substituting SBR 4601 with SBR 4602 in a silica-filled compound. This is higher than the difference in viscosity of the virgin materials, which is ~15 MU. This substantial increase in viscosity indicates that the functional part of SBR 4602 already interacts with the filler before curing has occurred. This adds resistance to the mobility of the polymer chains, which increases the force required to shear the material. Especially at high filler loadings, a ~30 MU increase can seriously limit processability of the compound. This could be remedied by addition of more processing aids, but this in turn could reduce the benefit of

using SBR 4602 in the first place. It is also of note that, due to the higher increase in viscosity, the Mooney viscosity of the virgin SBR 4602 is not fully indicative of the processability of the material when used in conjunction with a silica/silane filler system.

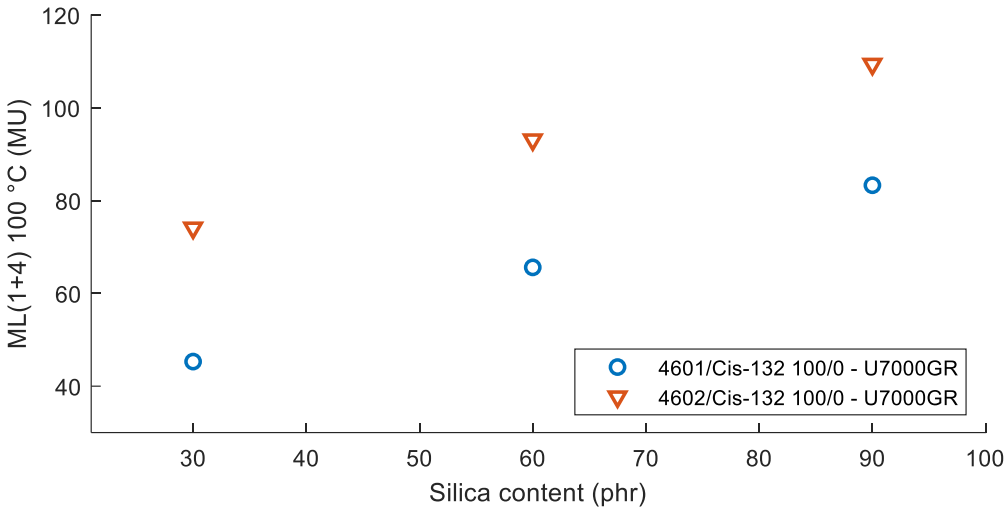

Figure 12: Mooney viscosity of compounds using pure SBR 4601 and SBR 4602.

Unvulcanized Payne effect

The unvulcanized Payne effect of compounds using pure SBR is shown in Table 6. Higher filler loadings show a higher Payne effect, as there is more material available to form a filler network making filler-filler interactions more probable. The Payne effect also increases when SBR 4601 is substituted by SBR 4602, which typically indicates worse micro-dispersion. However, some polymer-filler interaction can already occur due to the interaction between the functionalized end of the SBR 4602 and the silica particles [18]. This does not happen between SBR 4601 and silica, resulting in a reduced Payne-effect.

Table 6: Second sweep ΔG'(0.15%-100%) of pure SBR compounds.

			ΔG'(0.15%-100%) (kPa)		
Polymer	Blend	Silica type	30 phr	60 phr	90 phr
SBR 4601	100/0	U7000GR	340,96	501,96	601,61
SBR 4602	100/0	U7000GR	429,11	578,00	671,57

For a more complete image of the storage moduli, some selected results are shown in Figure 13 and Figure 14. Of note is the fact that at 100% strain, the lower plateau of the storage modulus has not been reached, so no claims can be made on any hydrodynamic effects, or the possibility of any in-rubber structure occurring before vulcanization. Figure 14 also shows that at high silica content, the filler network breaks down at a lower strain.

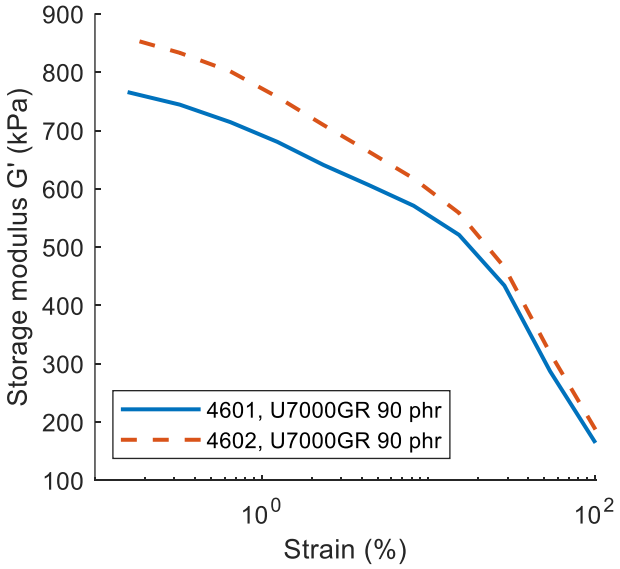

Figure 13: Second sweep storage modulus over strain of pure SBR 4601 and 4602, with 90 phr U7000GR silica.

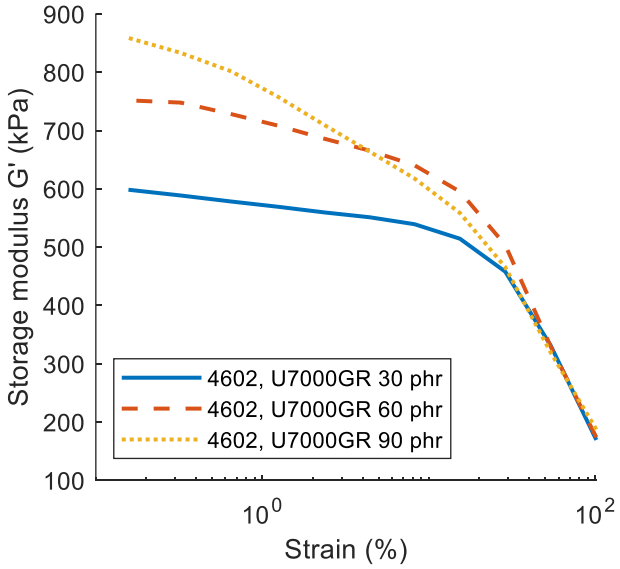

Figure 14: Second sweep storage modulus over strain of pure SBR 4602 compounds with varying content of U7000GR silica.

4.1.2 Vulcanization behavior

The curing data of compounds using pure SBR 4601 and SBR 4602 is shown in Table 7. As expected, the addition of silica increases minimum and maximum torque for both SBR types. Minimum torque increases when SBR 4601 is substituted by SBR 4602, which can be explained by the previously described interaction between silica and the functional group of SBR 4602. Scorch time is also slightly higher for compounds using SBR 4602. This could be caused by the interaction between the functional group and the zinc oxide-stearic acid complex, which are also needed in the curing reaction [29].

Table 7: Cure characteristics of pure SBR compounds.

			30 phr			60phr			90 phr		
Polymers	Blend	Silica	S'_{min}	S'_{max}	t_{scorch}	S'_{min}	S'_{max}	t_{scorch}	S'_{min}	S'_{max}	t_{scorch}
			(dNm)	(dNm)	(min)	(dNm)	(dNm)	(min)	(dNm)	(dNm)	(min)
4601/Cis-132	100/0	U7000GR	0,5	12,3	4,8	1,2	15,9	6,6	2,2	18,1	4,3
4602/Cis-132	100/0	U7000GR	1,6	13,4	5,2	2,5	15,9	7,0	3,3	18,1	4,3

Figure 15 shows a comparison between pure SBR 4601 and SBR 4602. It can be seen that the cure rate for SBR 4601 is significantly higher. Additionally, a more intense marching modulus is seen for compounds using SBR 4602. Both Table 7 and Figure 16 show that the scorch time for compounds with 90 phr silica is shorter than 60 phr silica content, which is unexpected. During mixing, accelerators are absorbed by the silica surface. When silica content is increased, more accelerators can be absorbed, delaying their effect during curing. This should increase scorch time and decrease cure rate. In this case, this holds true for 30 and 60 phr filler content. A working theory is that at 90 phr filler content, the percolation threshold is exceeded. This means a continuous filler network can be formed, which has a large impact on the torque measured during curing. This could affect the cure measurements, showing a “higher” cure rate.

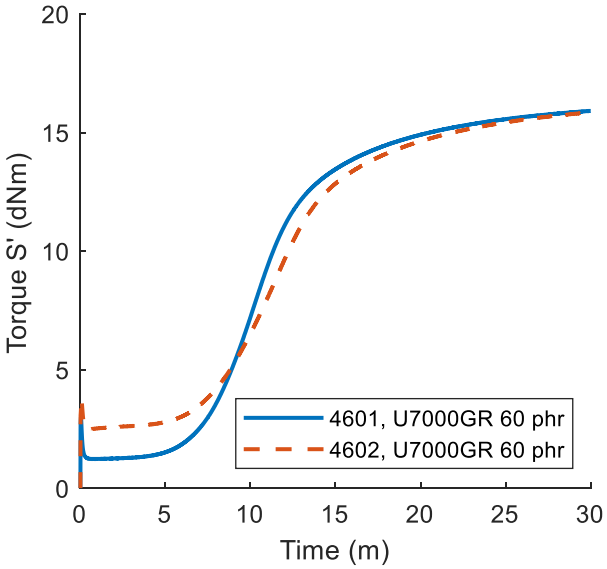

Figure 15: Cure curves of pure SBR compounds with 60 phr silica content.

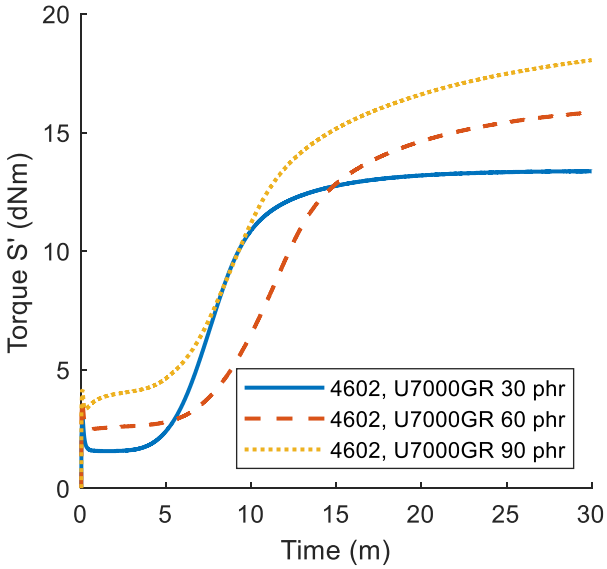

Figure 16: Cure curves of pure SBR 4602 compounds with varying silica content.

4.1.3 Mechanical behavior

Hardness

Hardness properties of the pure SBR compounds are shown in Figure 17. As can be seen, a near linear relation exists between hardness and filler content. No significant difference can be seen between the two SBR types.

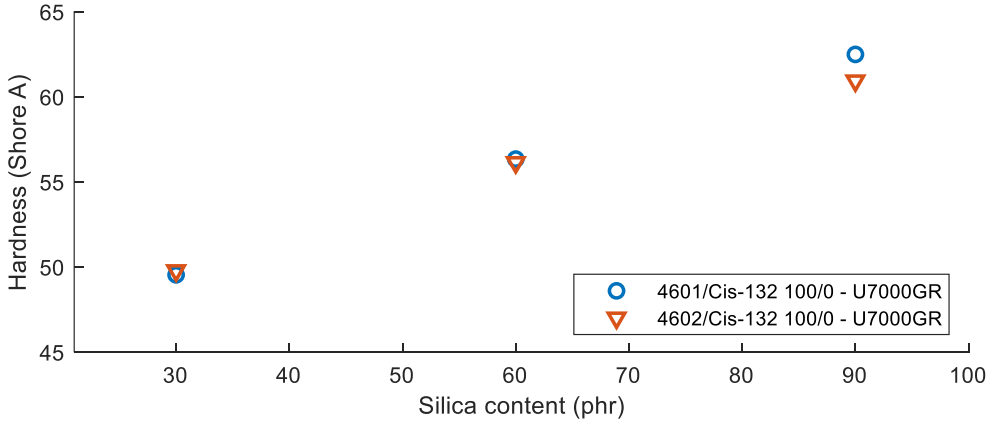

Figure 17: Hardness values of pure SBR compounds with varying silica content.

Stress-strain behavior

The mechanical properties of pure SBR compounds are shown in Table 8. Ultimate stress and strain properties show no significant differences, but the reinforcement index is slightly higher for compounds using SBR 4602, indicating that stress increases more rapidly at higher strains. This can be attributed to the functionalized group interacting with the silica particles in the compound, therefore including the chain ends in the spatial network, which increases the tensile strength.

Table 8: Mechanical properties of pure SBR compounds with 90 phr silica.

Polymers	Blend	Silica	$M_{100\%}$ (MPa)	$M_{300\%}$ (MPa)	M_{300}/M_{100}	σ_b (MPa)	ε_b (%)
4601/Cis-132	100/0	U7000GR	3,3	15,3	4,7	15,0	293
4602/Cis-132	100/0	U7000GR	2,9	16,0	5,5	15,9	298

The difference in reinforcement index is confirmed by Figure 18. In practical applications however, this is only a minute difference what will not have impact of the overall mechanical performance of the elastomer. Figure 19 shows the increase in reinforcement of the compound with increasing silica content, which is typical for a compound using a reinforcing filler.

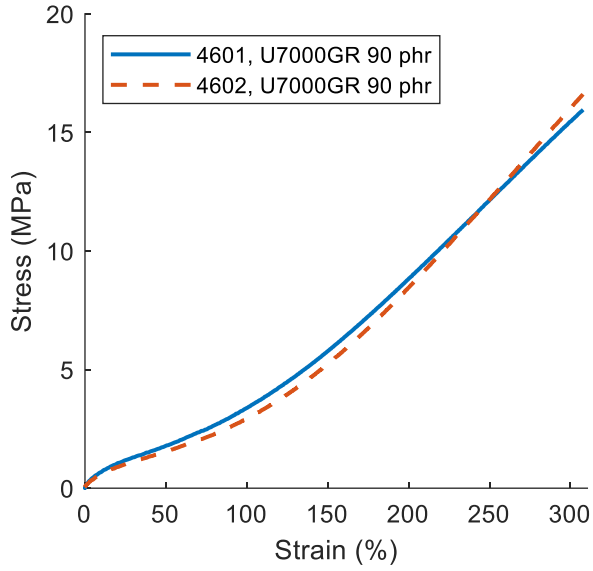

Figure 18: Stress-strain curve of pure SBR compounds, with 90 phr silica content.

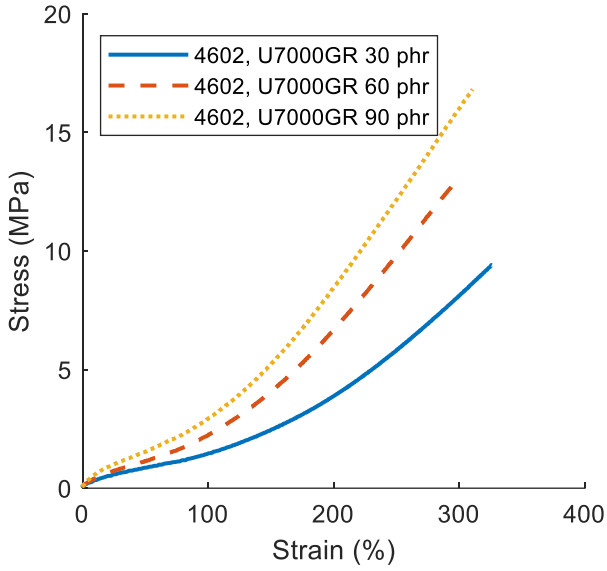

Figure 19: Stress-strain curve of pure SBR 4602 compounds, with varying silica content.

4.1.4 Dynamic behavior

Rebound

The rebound results for pure SBR compounds are shown in Figure 20. Here a strong relationship can be seen between hysteresis loss and silica loading. With higher filler loadings, the filler-filler interaction increases. This leads to more energy loss when deforming, as the filler structures in the polymer network are broken down, resulting in a lower rebound value [20]. At room temperature, no significant difference in rebound can be seen between SBR 4601 and SBR 4602.

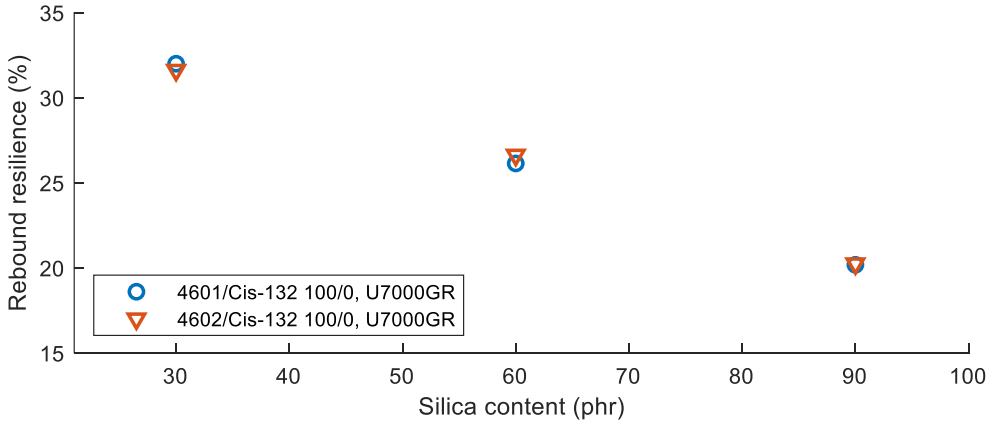

Figure 20: Room temperature rebound resilience of pure SBR compounds.

Dynamic Mechanical Analysis

Figure 21 shows the loss angle curve of the pure SBR compounds at 60 phr filler content. Both SBR 4601 and SBR 4602 have similar glass transition temperatures, but the tan(δ) values differ, with SBR 4602 having a slightly higher tan(δ), indicating the functionalized group reduces the relative elasticity of the polymer chain at T_g. Around 0 °C and room temperature, loss angles are similar between both SBR types, indicating similar wet grip performance and validating the findings in the previous section. At 60 °C, the SBR 4602 shows slightly lower loss angles compared to SBR 4601. This can be attributed to the end-functionalization interacting with the filler system, reducing the amount of free chain ends compared to non-functionalized elastomers. This reduces hysteresis, reducing rolling resistance.

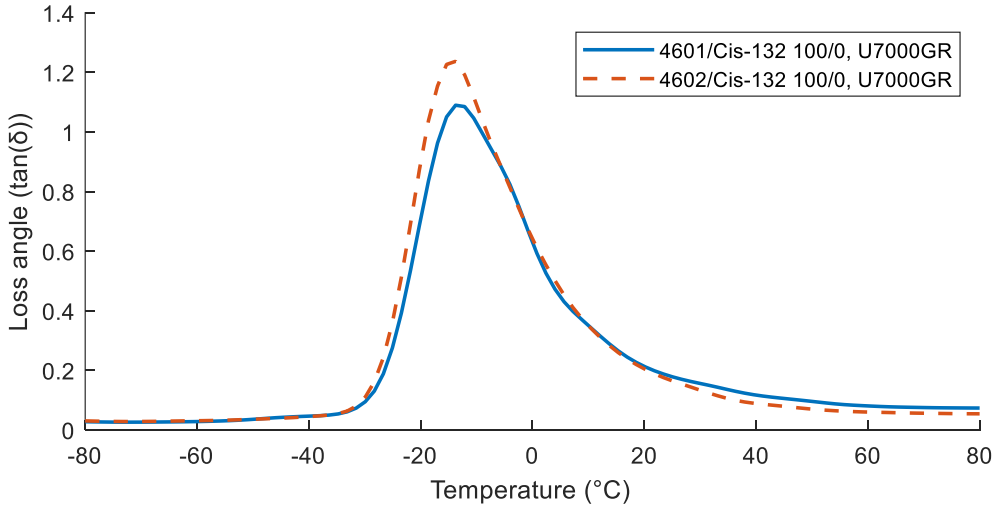

Figure 21: DMA curve of pure SBR compounds with 60 phr silica content.

4.2 Series 2: SBR/BR blends, varying BR type

4.2.1 Processability

Mixing curves

When using a blend with SBR and BR in an 80/20 ratio, the difference in rotor torque and temperature increase are similar to what is discussed in Section 4.1.1. regarding the difference between SBR 4601 and SBR 4602. However, it can be seen in Figure 22 that the difference between SBR 4601 and 4602 is somewhat dampened due to the introduction of another (non-functionalized) polymer. This means that the contribution of SBR 4602 to the increase in rotor torque and increase in temperature is decreased. A more significant difference between BR Cis-132 and BR CB-24 can be seen, as the compound using BR CB-24 reaches higher temperatures at similar rotor torque to the compound using BR Cis-132. However, this difference can be attributed to operator error, as compounds using different blends were mixed on different days.

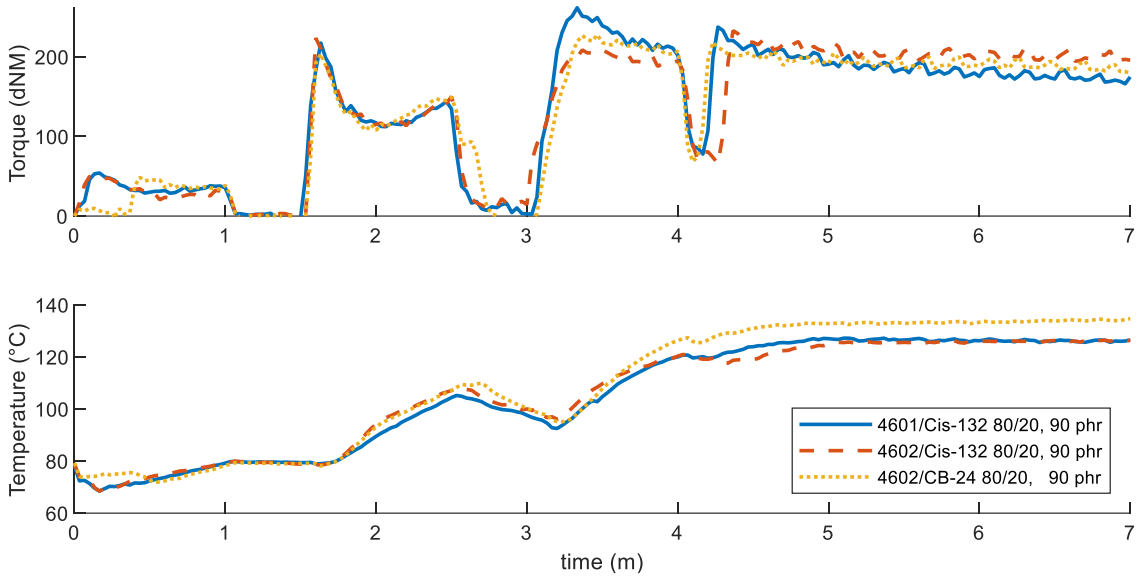

Figure 22: Torque and temperature, first mixing stage SBR/BR blends comparing BR types.

Mooney viscosity

As can be seen in Figure 23, the variation of BR type does not influence the viscosity of the compounds significantly. The viscosity of blends using BR CB-24 is slightly higher than blends using BR Cis-132 for all amounts of filler, but not significantly. This is expected, as both types of BR vary only slightly in cis-content and possibly have only slight differences in branching. Again, the largest influence on viscosity is the variation between SBR types.

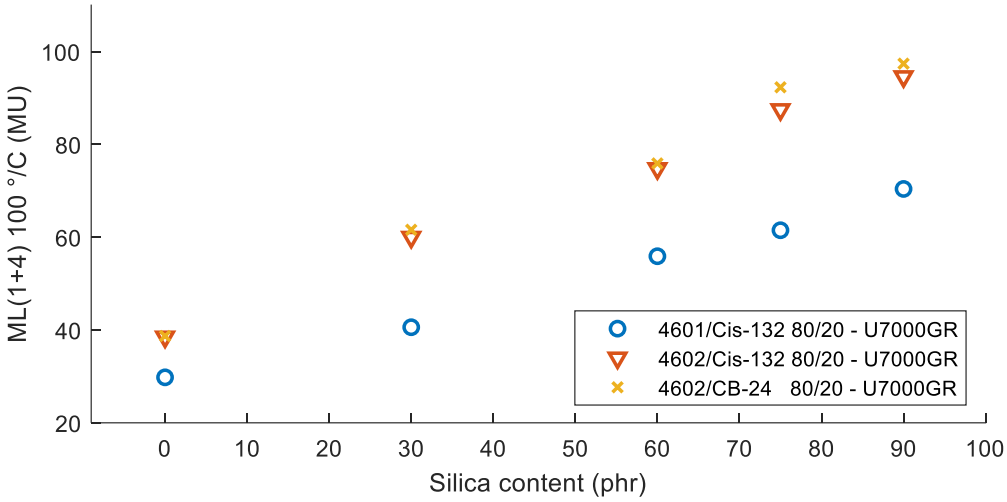

Figure 23: Mooney viscosity of compounds using blends of SBR and BR with varying BR types.

Unvulcanized Payne effect

The unvulcanized Payne effect of compounds using SBR/BR blends is shown in Table 9. The Payne effect for unfilled SBR 4601 / BR Cis-132 compound shows slightly higher values than the compounds using SBR 4602 / BR Cis-132, probably because of the small amount of carbon black that interacts with the functionalized chain end of SBR 4601. Elsewhere, the ΔG' is higher for the compounds using SBR 4602 as there is a probable interaction between the silica and functionalized chain end of the SBR 4602. The difference in ΔG' between the compounds using BR CB-24 and BR Cis-132 are smaller. BR Cis-132 shows slightly higher Payne effect and as both BR types are non-functionalized, this can indicate that compounds using a SBR 4602 / BR CB-24 blend have slightly better micro-dispersion.

Table 9: Second sweep ΔG' of SBR/BR blends with varying SBR and BR types.

Polymers	Blend	Silica type	ΔG'(0.15%-100%) (kPa)				
			0 phr	30 phr	60 phr	75 phr	90 phr
4601/Cis-132	80/20	U7000GR	156,23	354,53	457,18	570,75	620,49
4602/Cis-132	80/20	U7000GR	132,05	320,77	434,25	539,54	665,06
4602/CB-24	80/20	U7000GR	128,56	272,64	388,34	469,61	531,30

Some selected storage modulus/strain of compounds using varying SBR/BR blends are shown in Figure 24 and Figure 25. For both compounds using BR CB-24 and BR Cis-132, G'(100%) shows no significant difference at both 60 and 90 phr silica this indicates that the magnitude of hydrodynamic effects are most likely similar between the two compounds.

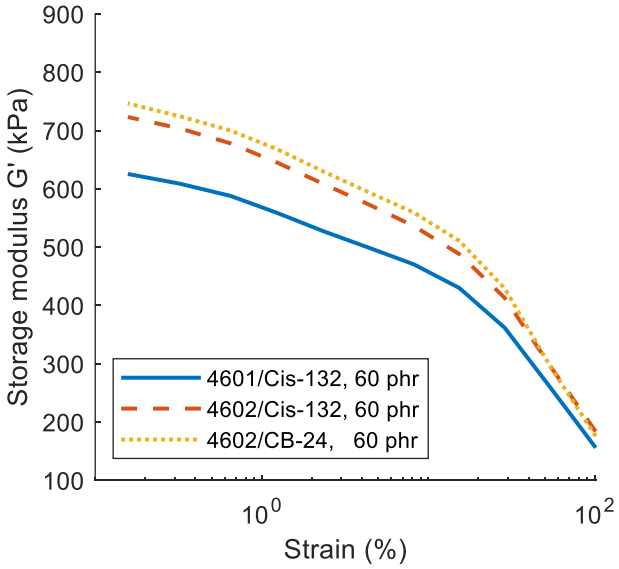

Figure 24: Second sweep storage modulus over strain of SBR/BR compounds in 80/20 blend with 60 phr of U7000GR silica.

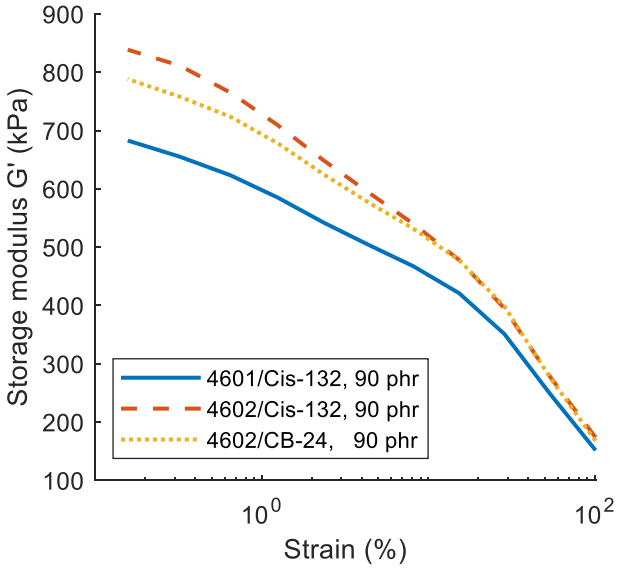

Figure 25: Second sweep storage modulus over strain of SBR/BR compounds in 80/20 blend with 90 phr of U7000GR silica.

4.2.2 Vulcanization behavior

The curing data of compounds using SBR/BR blends is shown in Table 10. Again, S'_{min} is lower for compounds using SBR 4601 relative to compounds using SBR 4602. S'_{max} reaches slightly lower values as well. For all silica contents except 90 phr, scorch time increases with the use of BR CB-24 compared to compounds using BR Cis-132. This is unexpected, as both BR types are fairly similar according to the raw material data in Table 1 and therefore are expected to have similar cure characteristics.

Table 10: Cure characteristics of various SBR/BR blends.

			0 phr			30 phr			60phr		
Polymers	Blend	Silica	S'_{min} (dNm)	S'_{max} (dNm)	t_{scorch} (min)	S'_{min} (dNm)	S'_{max} (dNm)	t_{scorch} (min)	S'_{min} (dNm)	S'_{max} (dNm)	t_{scorch} (min)
4601/Cis-132	80/20	U7000GR	0,4	9,1	2,6	0,7	13,3	4,7	1,4	16,8	6,0
4602/Cis-132	80/20	U7000GR	0,6	9,5	2,9	1,4	14,0	4,8	2,4	16,3	6,3
4602/CB-24	80/20	U7000GR	0,6	9,4	3,1	1,5	14,2	5,6	2,2	16,4	7,1
			75 phr			90 phr					
Polymers	Blend	Silica	S'_{min} (dNm)	S'_{max} (dNm)	t_{scorch} (min)	S'_{min} (dNm)	S'_{max} (dNm)	t_{scorch} (min)			
4601/Cis-132	80/20	U7000GR	1,9	18,8	4,8	2,5	18,0	1,6			
4602/Cis-132	80/20	U7000GR	3,4	19,5	3,8	4,3	21,0	2,6			
4602/CB-24	80/20	U7000GR	3,0	19,0	5,3	3,4	19,2	1,6			

Figure 26 shows the cure curves of SBR/BR blends with 60 phr filler content. The compound using BR CB-24 shows, in addition to the longer scorch time, a lower crosslinking rate. A higher marching modulus intensity is seen, resulting in a similar S'_{max} compared to compounds using BR Cis-132. As described previously, the crosslinking rate for the compounds using SBR 4601 is higher, but reaches similar peak torque as compounds using SBR 4602, with similar marching modulus intensity.

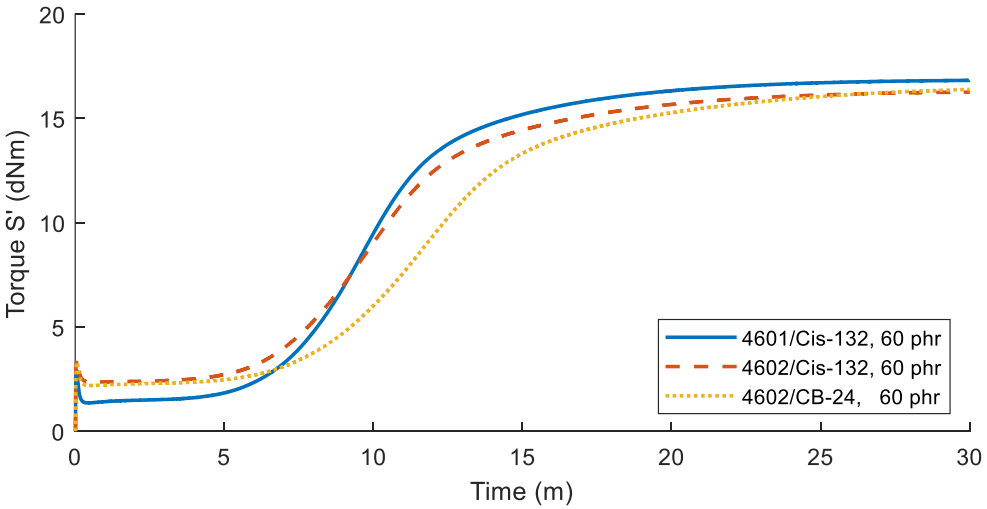

Figure 26: Cure curves of compounds with various SBR/BR blends and 60 phr silica content.

4.2.3 Mechanical behavior

Hardness

Figure 27 shows again that variation in elastomer type does not significantly affect the hardness properties of a compound and there is a positive linear relationship between hardness and filler content.

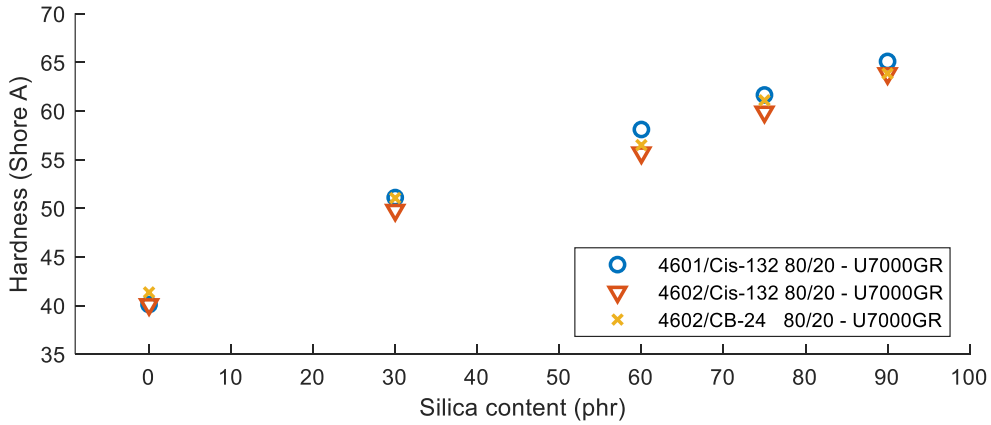

Figure 27: Hardness values of varying SBR/BR blends with varying silica content.

Stress-strain behavior

The mechanical properties of SBR/BR blends with varying BR types is shown in Table 11. With the two BR types having fairly similar characteristics, mechanical behavior of BR Cis-132 and BR CB-24 is similar. Again, compounds using SBR 4602 show slightly higher reinforcement compared to compounds using SBR 4601. Elsewhere, no significant differences are found in the mechanical properties of this series.

Table 11: Mechanical properties of compounds with SBR/BR blends, varying SBR and BR type, containing 90 phr of Silica.

Polymers	Blend	Silica	$M_{100\%}$ (MPa)	$M_{300\%}$ (MPa)	M_{300}/M_{100}	σ_b (MPa)	ε_b (%)
4601/Cis-132	80/20	U7000GR	3,1	13,1	4,2	14,5	325
4602/Cis-132	80/20	U7000GR	2,8	14,0	5,1	12,9	280
4602/CB-24	80/20	U7000GR	2,9	13,9	4,9	16,0	335

4.2.4 Dynamic behavior

Rebound

Figure 28 shows the rebound at room temperature of various SBR/BR compounds. All blends show slightly different values, with the SBR 4601/ BR Cis-132 compound showing the lowest rebound and the SBR 4602 / BR CB-24 showing the highest rebound. Most likely, this is because BR CB-24 has a less branched structure compared to BR Cis-132, meaning there are less free chain ends causing hysteresis, resulting in a higher rebound resilience.

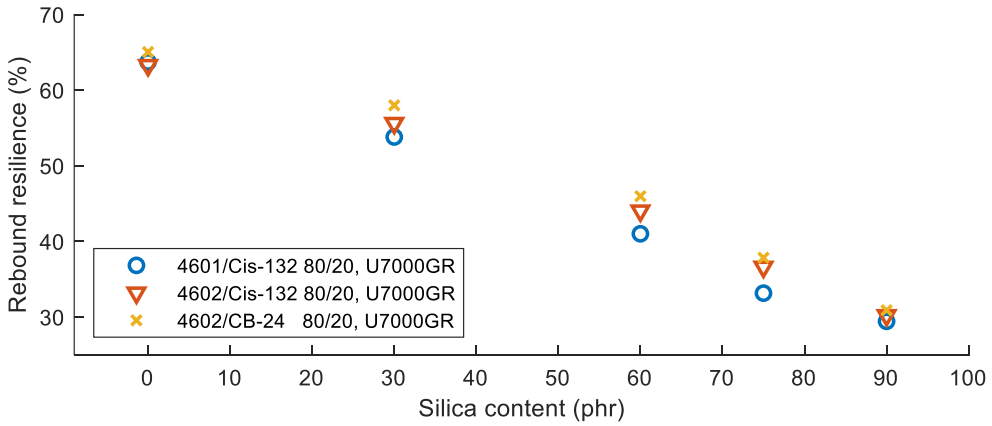

Figure 28: Room temperature rebound resilience of varying SBR/BR blends.

Dynamic Mechanical Analysis

Figure 29 shows the loss angle curve of SBR/BR blends with varying SBR and BR type. The glass transition temperature of both compounds using SBR 4602 is similar, as well as the tan(δ) values. This is expected, as both BR types have a similar T_g. The SBR 4601 / BR Cis-132 compound shows a lower T_g, which is unexpected and not consistent with the data from the previous series. Therefore, its tan(δ) values will be disregarded in further analysis. At 0 °C, tan(δ) values for both compounds using SBR 4602 are similar, indicating similar wet grip properties. At 60 °C, tan(δ) values for the 4602/Cis-132 compound are slightly lower, indicating slightly better rolling resistance properties.

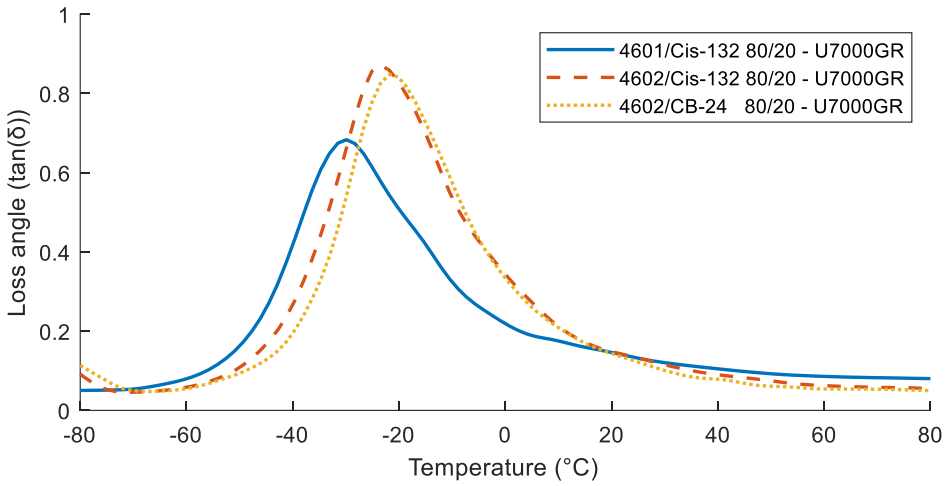

Figure 29: DMA curve of varying SBR/BR blends with 60 phr silica content.

4.3 Series 3: SBR/BR blends, varying blend ratio

4.3.1 Processability

Mixing curves

Although BR Cis-132 has a lower viscosity than SBR 4602, the temperature and rotor torque do not change significantly during all mixing stages when added to the compound in 100/0, 80/20, and 60/40 ratios. As can be seen in Figure 30, compounds that use 100% SBR 4602 tend to heat up slightly quicker, but converge to similar temperatures towards the end of all mixing stages. Any large differences in torque and temperature can be attributed to human error, since temperature management during isothermal mixing is done by adjusting (lowering) rotor speed manually. From a mixing perspective, processing does slightly improve when SBR 4602 is blended with BR Cis-132.

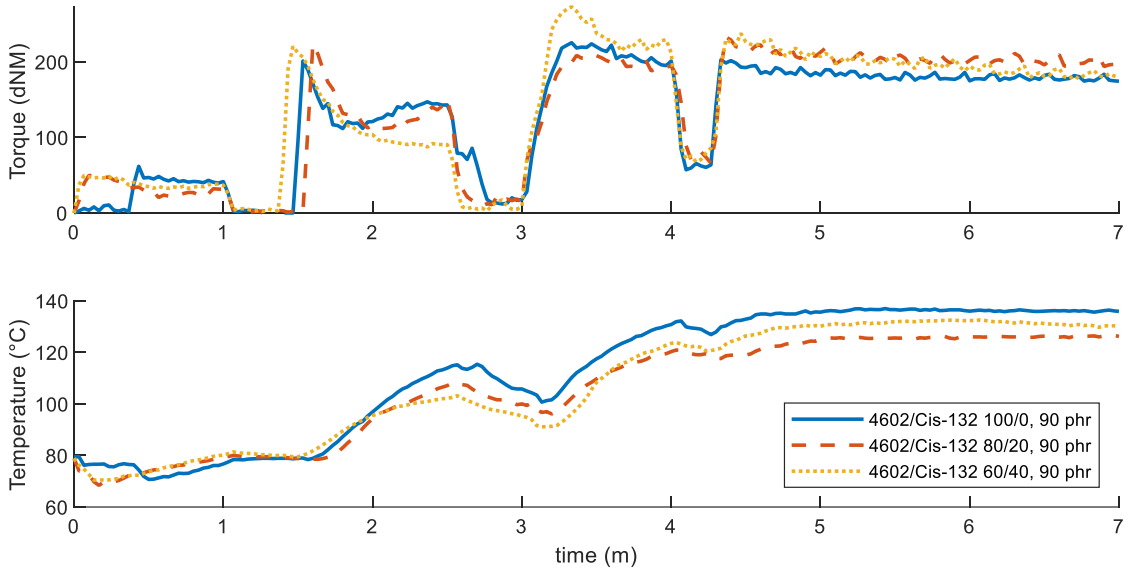

Figure 30: Torque and temperature, first mixing stage, 4602/Cis-132 blends with varying blend ratios.

Mooney viscosity

The Mooney viscosities of compounds using varying blend ratios of SBR 4602 and BR Cis-132 are shown in Figure 31. As expected, the addition of the lower viscosity BR Cis-132 lowers the viscosity of the compounds over all filler contents. Compared to pure SBR 4602, the viscosity drops with ~15 MU and ~25 MU when using an 80/20 and a 60/40 SBR 4602 / BR Cis-132 blend respectively. The viscosity lowers with the increase of BR Cis-132. This again supports the finding from the previous section that processability is improved when an SBR/BR blend is used. With the improved processability, it will be more feasible to compound rubbers with high filler content compared to pure SBR compounds. However, dynamic properties will change with adjustment of the SBR/BR blend ratio.

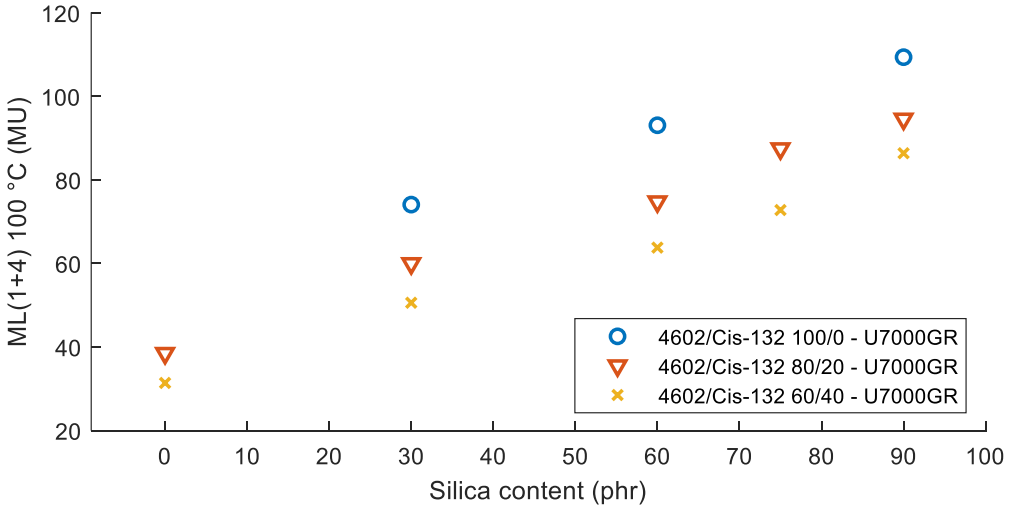

Figure 31: Mooney viscosity of compounds using varying blend ratios of SBR 4602 and Cis-132.

Unvulcanized Payne effect

The unvulcanized Payne effect of compounds using SBR 4602 / BR Cis-132 in varying blend ratios is shown in Table 12. Visible is the decrease in Payne effect with decreasing SBR content. Dispersion quality cannot be indicated, as there is a decreasing amount of functionalized polymer with an increasing amount of BR content.

Table 12: Second sweep ΔG' of SBR 4602 / Cis-132 blends with varying blend ratios.

			ΔG'(0.15%-100%) (kPa)				
Polymers	Blend	Silica type	0 phr	30 phr	60 phr	75 phr	90 phr
4602/Cis-132	100/0	U7000GR		429,11	578,00		671,57
4602/Cis-132	80/20	U7000GR	132,05	320,77	434,25	539,54	665,06
4602/Cis-132	60/40	U7000GR	106,40	248,69	331,88	403,94	543,64

Some selected storage modulus/strain of compounds using varying SBR/BR blends are shown in Figure 32 and Figure 33. Regardless of BR content, the slope of the filler breakdown is steeper for compounds with 90 phr silica. The relatively high Payne effect of the compound with SBR/BR ratio 80/20 and 90 phr silica (Figure 33) can be attributed to a lack of silanization as the mixing temperature was relatively low (Figure 30). As can be seen in Figure 32, the Payne effect at other silica contents is more as expected.

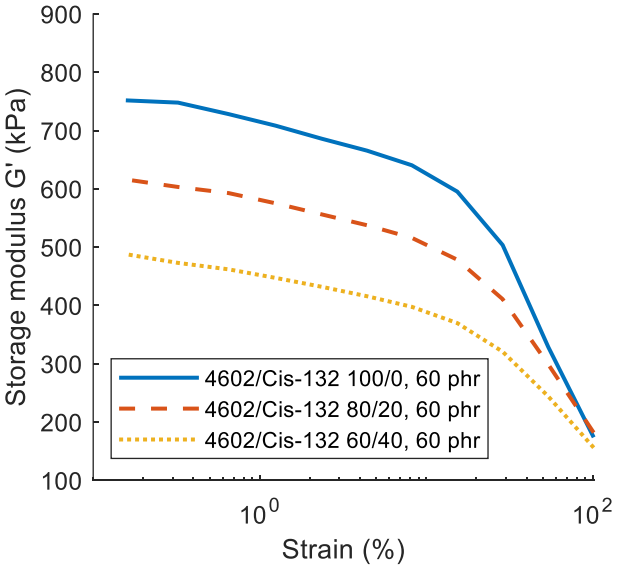

Figure 32: Second sweep storage modulus over strain of SBR 4602 / BR Cis-132 compounds with varying blend ratios, with 90 phr U7000GR silica.

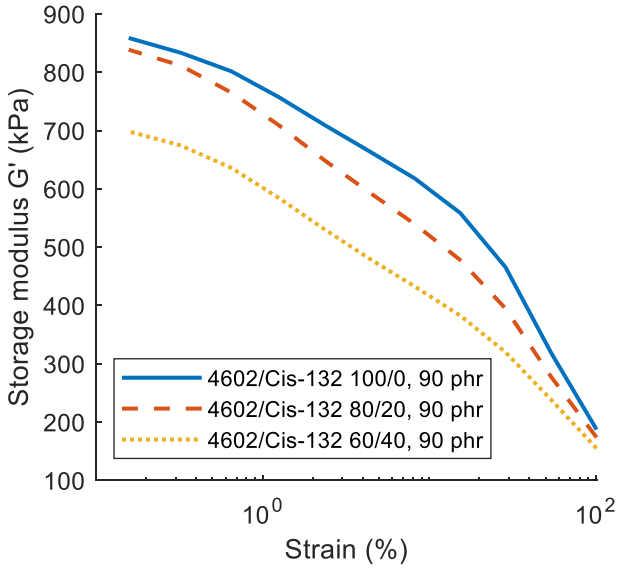

Figure 33: Second sweep storage modulus over strain of SBR 4602 / BR Cis-132 compounds with varying blend ratios, with 90 phr U7000GR silica.

4.3.2 Vulcanization behavior

The cure characteristics of SBR/BR blends with varying blend ratios is shown in Table 13. For all compounds except for the compound using 75 phr silica, the scorch time decreases and the cure rate increases with increasing BR content, as BR has a higher amount of reactive double bonds compared to SBR. Additionally, the high amount of cis-content in BR Cis-132 has the potential to speed up the vulcanization reaction, as these cis-configurations have higher reactivity compared to vinyl configurations [57]. In addition to shorter scorch times, Figure 34 shows higher cure rates and a lower marching modulus intensity with increasing BR content.

Table 13: Cure characteristics of SBR/BR blends with varying blend ratios.

			0 phr			30 phr			60phr		
Polymers	Blend	Silica	S'_{min}	S'_{max}	t_{scorch}	S'_{min}	S'_{max}	t_{scorch}	S'_{min}	S'_{max}	t_{scorch}
			(dNm)	(dNm)	(min)	(dNm)	(dNm)	(min)	(dNm)	(dNm)	(min)
4602/Cis-132	100/0	U7000GR				1,6	13,4	5,2	2,5	15,9	7,0
4602/Cis-132	80/20	U7000GR	0,6	9,5	2,9	1,4	14,0	4,8	2,4	16,3	6,3
4602/Cis-132	60/40	U7000GR	0,6	10,0	2,6	1,3	14,6	4,5	2,0	15,9	5,9
			75 phr			90 phr					
Polymers	Blend	Silica	S'_{min}	S'_{max}	t_{scorch}	S'_{min}	S'_{max}	t_{scorch}			
			(dNm)	(dNm)	(min)	(dNm)	(dNm)	(min)			
4602/Cis-132	100/0	U7000GR				3,3	18,1	4,3			
4602/Cis-132	80/20	U7000GR	3,4	19,5	3,8	4,3	21,0	2,6			
4602/Cis-132	60/40	U7000GR	2,6	17,7	4,5	3,7	19,7	1,1			

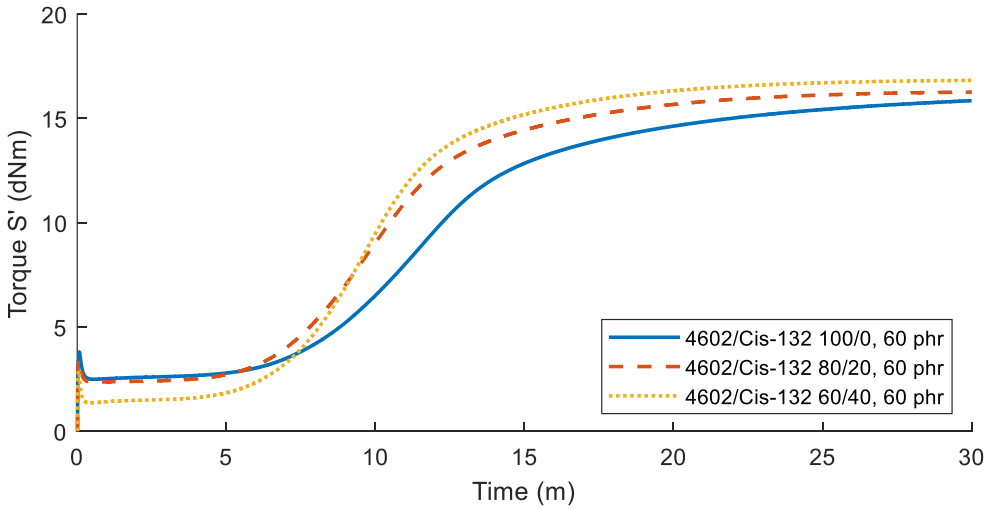

Figure 34: Cure curves of compounds with SBR 4602 / BR Cis-132 in varying blend ratios and 60 phr silica content.

4.3.3 Mechanical behavior

Hardness

Figure 35 shows the hardness values of SBR 4602 / BR Cis-132 blends with varying blend ratios. Hardness properties are not affected by changing the blend ratio, with only the silica content dictating the hardness values. Again, a linear increase in hardness is recorded with an increase in silica content.

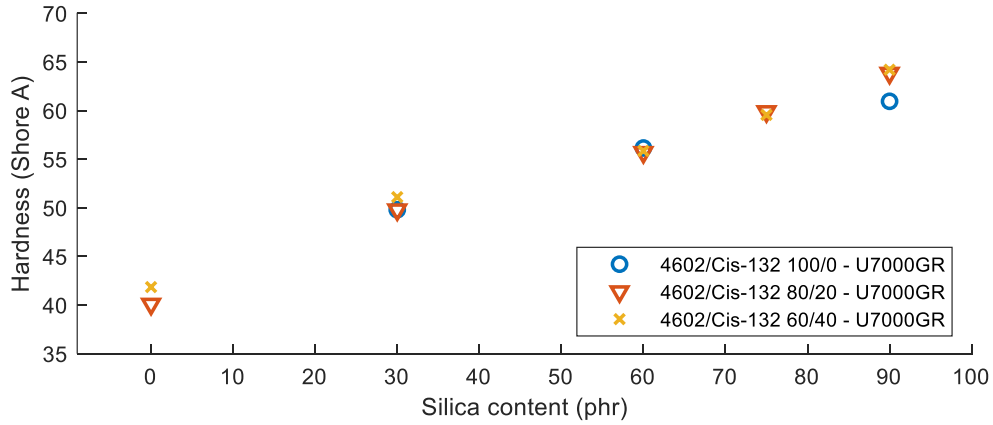

Figure 35: Hardness values of SBR 4602 / BR Cis-132 blends with varying blend ratios.

Stress-strain behavior

The mechanical properties of SBR 4602 / BR Cis-132 blends with varying blend ratios is shown in

Table 14. Here, the difference in mechanical properties can clearly be seen. Mainly due to the styrene group present in SBR, chain mobility is limited. This results in a higher stress at a given strain. BR does not have styrene groups, and therefore shows lower stresses at a given strain.

Table 14: Mechanical properties of SBR 4602 / BR Cis-132 compounds with varying blend ratios, using 90 phr silica.

Polymers	Blend	Silica	$M_{100\%}$ (MPa)	$M_{300\%}$ (MPa)	M_{300}/M_{100}	σ_b (MPa)	ε_b (%)
4602/Cis-132	100/0	U7000GR	2,9	16,0	5,5	15,9	298
4602/Cis-132	80/20	U7000GR	2,8	14,0	5,1	12,9	280
4602/Cis-132	60/40	U7000GR	2,6	11,3	4,4	15,2	368

The difference in mechanical properties between different blend ratios is graphically represented in Figure 36. This shows that only minor adjustments in the blend ratio can have large impact on mechanical performance of the tire tread compound.

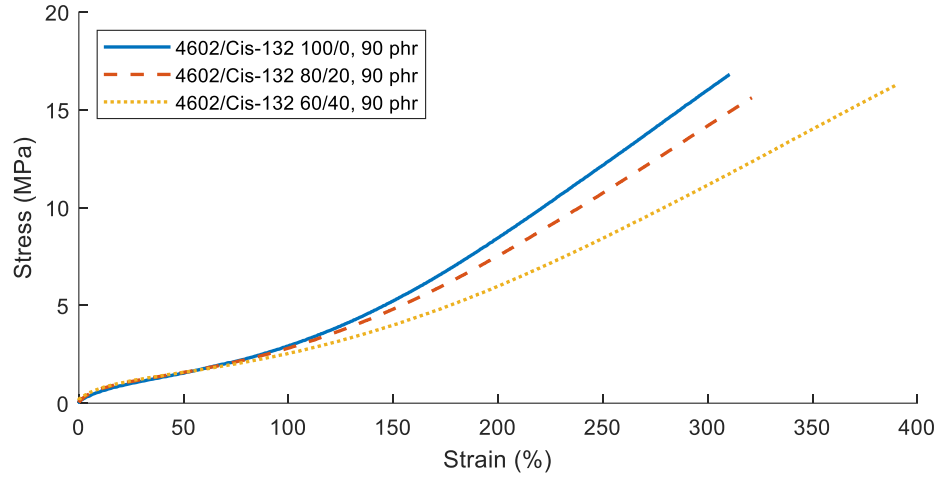

Figure 36: Stress-strain curve of SBR 4602 / BR Cis-132 compounds, with varying blend ratios, with 90 phr silica content.

4.3.4 Dynamic behavior

Rebound

The rebound results for SBR 4602 / BR Cis-132 compounds with varying blend ratios is shown in Figure 37. BR Cis-132 has high cis-content and shows high rebound properties. On the other hand, the styrene group of SBR 4602 increases the T_g and subsequently deteriorates the rebound properties. This is also visible in Figure 37, as rebound significantly decreases for all silica contents with increasing SBR 4602 content.

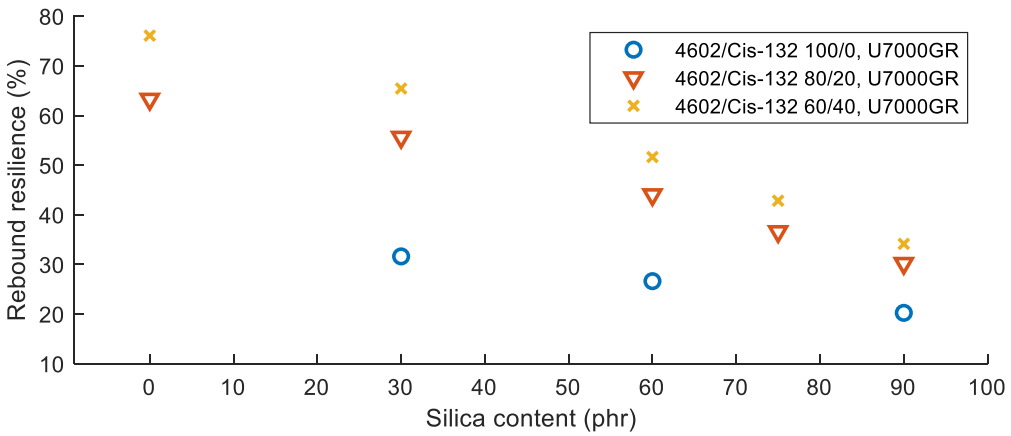

Figure 37: Room temperature rebound resilience of SBR 4602 / BR Cis-132 blends with varying blend ratio.

Dynamic Mechanical Analysis

Figure 38 shows the loss angle curve of SBR 4602 / BR Cis-132 compounds with varying blend ratio. The glass transition temperature as well as the tan(δ) value at T_g decreases with increasing BR content. This shift in T_g indicates improvement in tread wear performance of the tire tread compound with increasing BR content. Due to the T_g shift, the tan(δ) value at 0 °C decreases significantly with increasing BR content, negatively impacting the wet grip performance. Loss angle values at room temperature are consistent with the rebound data, with the highest tan(δ) values for the pure SBR compound. At 60 °C, the tan(δ) value increases slightly with increasing BR content, indicating a slight increase in rolling resistance. Typically, the increase of the BR fraction improves rolling resistance in a tire tread compound using a SBR/BR blend.

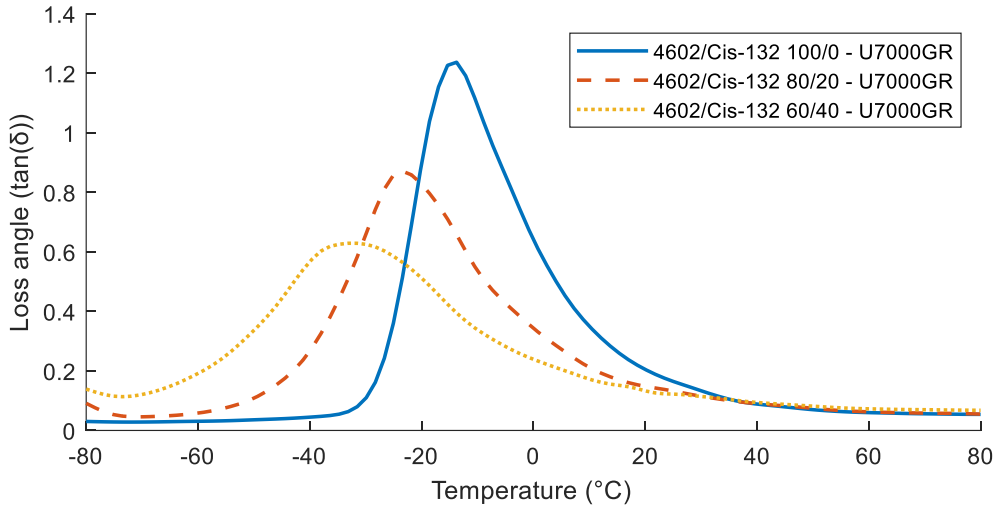

Figure 38: DMA curve of SBR 4602 / BR Cis-132 blends, varying blend ratio, with 60 phr silica content.

4.4 Series 4: SBR/BR blends, varying silica type

4.4.1 Processability

Mixing curves

When varying the silica specific surface area, the rotor torque and temperature increases with increasing surface area, as can be seen in Figure 39. This is expected, as the increase in specific surface area in turn increases the interaction between polymer and filler. When compounding a high SSA silica with the functionalized SBR 4602, temperature management becomes increasingly difficult, especially at high (75 phr and up) silica loadings. This improves marginally when substituting SBR 4602 with SBR 4601. In contrast, temperature management improves with the use of low SSA silica, making it more suitable for combination with SBR 4602.

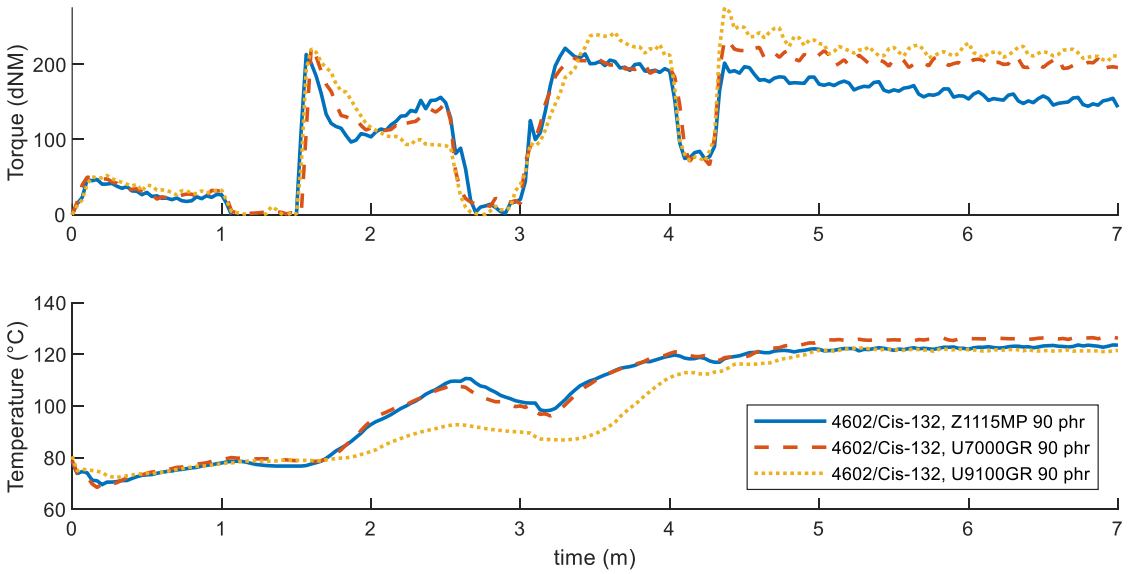

Figure 39: Torque and temperature, 1st mixing stage, 4602/Cis-132 blends with varying silica SSA, using 90 phr silica.

Mooney viscosity

The Mooney viscosities of compounds using silicas with varying surface areas are shown in Figure 40. The usage of high SSA silica (U9100GR) increases viscosity of the compounds significantly, as the higher amount of surface area increases the polymer-filler interaction, increasing shear forces. The opposite happens when using a low SSA silica (Z1115MP). Here, less of the silica surface is available to interact with the polymer, reducing required forces to shear the material. With the increased viscosity of high SSA silica, processability at high filler content deteriorates significantly to the point that, even with an SBR/BR blend, issues will almost certainly arise when mixing. On the other hand, low SSA compounds could profit from the increased viscosity of SBR 4602 to improve internal shear forces when mixing.

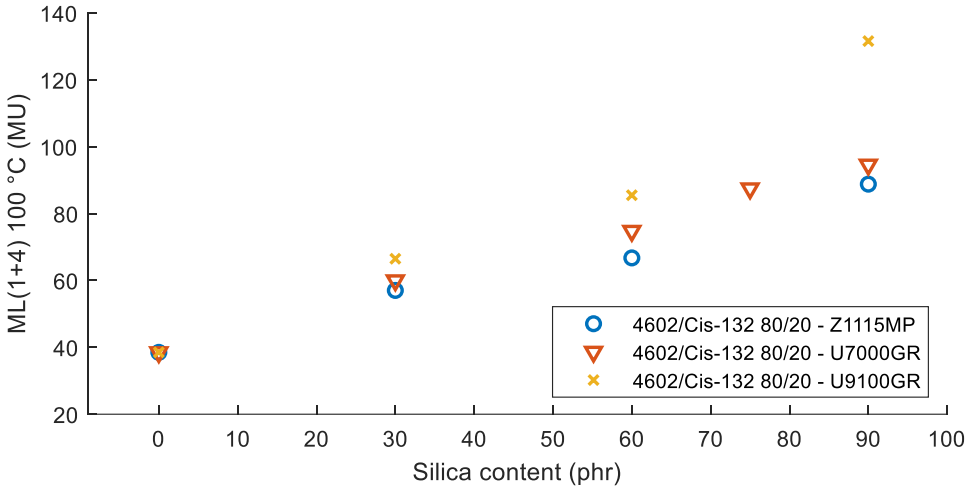

Figure 40: Mooney viscosity of compounds using silicas with varying surface areas.

Unvulcanized Payne effect

The unvulcanized Payne effect of compounds using SBR/BR blends with varying silica surface areas is shown in Table 15. A clear difference in ΔG' can be seen between

compounds using silica U7000GR and U9100GR, when comparing both SBR 4601 and SBR 4602. This is expected, as silica U9100GR has a higher SSA, which makes the probability of forming a filler network higher. For the same reason a lower ΔG' was expected for the lower SSA silica Z1115MP, but as can be seen in Table 15, slightly higher ΔG' values than silica U7000GR are recorded for 30 and 60 phr silica content. This could be explained by the difference between granulated and micro-pearl silica showing different magnitudes in Payne effect. Again, ΔG' increases for all types of silica when substituting SBR 4601 with SBR 4602 due to the interaction between the silica and the chain-end functionalization. This increase in ΔG' is exaggerated when combining the effects of a high silica content, high silica SSA, and filler-polymer interaction.

Table 15: Second sweep ΔG' of SBR/BR blends with varying silica types.

			ΔG'(0.15%-100%) (kPa)				
Polymers	Blend	Silica type	0 phr	30 phr	60 phr	75 phr	90 phr
4601/Cis-132	80/20	Z1115MP		268,53	399,33		473,21
4602/Cis-132	80/20	Z1115MP		336,55	446,29		661,49
4601/Cis-132	80/20	U7000GR	128,56	272,64	388,34	469,61	531,30
4602/Cis-132	80/20	U7000GR	132,05	320,77	434,25	539,54	665,06
4601/Cis-132	80/20	U9100GR		344,86	527,19		964,53
4602/Cis-132	80/20	U9100GR		401,14	542,27		1270,67

Some selected storage moduli/strains of compounds using silica types combined with an SBR 4601 / BR Cis-132 blend and an SBR 4602 / BR Cis-132 blend are shown in Figure 41 and Figure 42, respectively. As can be seen, the difference in Payne-effect between compounds using silica Z1115MP and U7000GR negligible, but the trajectory of the curve is slightly different. This indicates that filler network breakdown happens at a different rate between the two silica types.

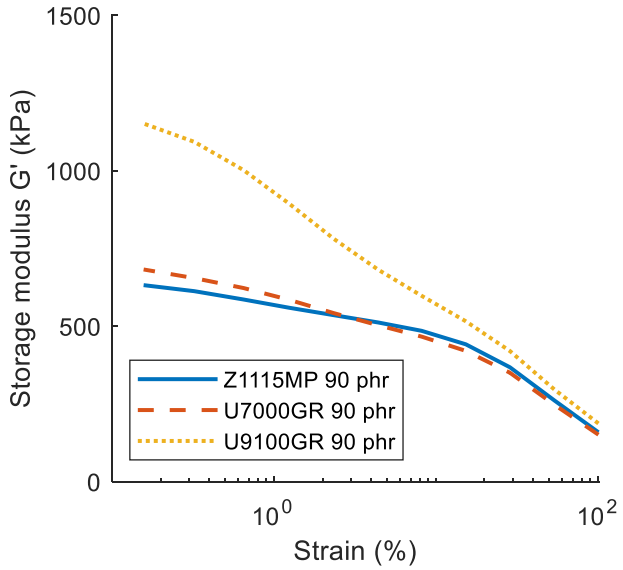

Figure 41: Second sweep storage modulus over strain of SBR 4601/BR Cis-132 compounds blended in an 80/20 ratio, with 90 phr of varying silica types.

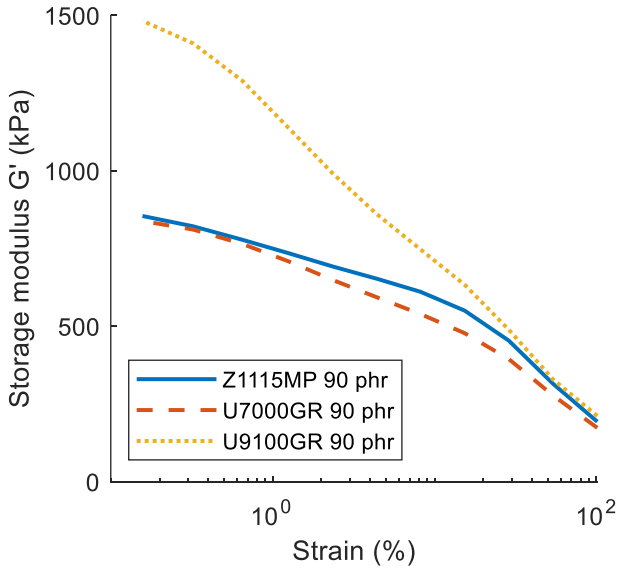

Figure 42: Second sweep storage modulus over strain of SBR 4602/BR Cis-132 compounds blended in an 80/20 ratio, with 90 phr of varying silica types.

4.4.2 Vulcanization behavior

Table 16 shows the cure characteristics of SBR/BR blends with varying silica types and loadings. Both the high SSA and low SSA silica seem to reduce scorch time significantly compared to the medium SSA silica. Additionally, the crosslinking rate increases for both high and low SSA. This can be attributed to the same theory presented in Section 4.1.2, with low SSA silica having less surface to absorb accelerators, and high SSA silica exceeding the percolation threshold. Similar S'_{max} is reached between low and medium SSA compounds, but with low SSA compounds showing a reduced degree of marching modulus intensity.

Table 16: Cure characteristics of SBR/BR blends with varying silica types.

			30 phr			60phr			90 phr		
Polymers	Blend	Silica	S'_{min} (dNm)	S'_{max} (dNm)	t_{scorch} (min)	S'_{min} (dNm)	S'_{max} (dNm)	t_{scorch} (min)	S'_{min} (dNm)	S'_{max} (dNm)	t_{scorch} (min)
4601/Cis-132	80/20	Z1115MP	0,6	14,0	3,3	1,0	17,6	3,9	1,9	20,5	3,4
4602/Cis-132	80/20	Z1115MP	1,4	14,1	3,9	1,9	16,9	4,4	3,3	21,5	3,3
4601/Cis-132	80/20	U7000GR	0,7	13,3	4,7	1,4	16,8	6,0	2,5	18,0	1,6
4602/Cis-132	80/20	U7000GR	1,4	14,0	4,8	2,4	16,3	6,3	4,3	21,0	2,6
4601/Cis-132	80/20	U9100GR	1,0	15,3	4,2	2,3	20,2	4,0	4,6	23,4	0,2
4602/Cis-132	80/20	U9100GR	1,8	15,7	4,8	3,2	19,0	4,5	5,8	27,7	0,1

For all almost all silica types and loadings, an increase in scorch time is seen when substituting SBR 4601 with SBR 4602, which is consistent with the findings shown in the previous series. Figure 43 and Figure 44 both show the cure curves for SBR 4601 / BR Cis-132 and SBR 4602 / BR Cis-132, respectively. The higher cure rate and shorter scorch time at low and high silica SSA is visible for both SBR types.

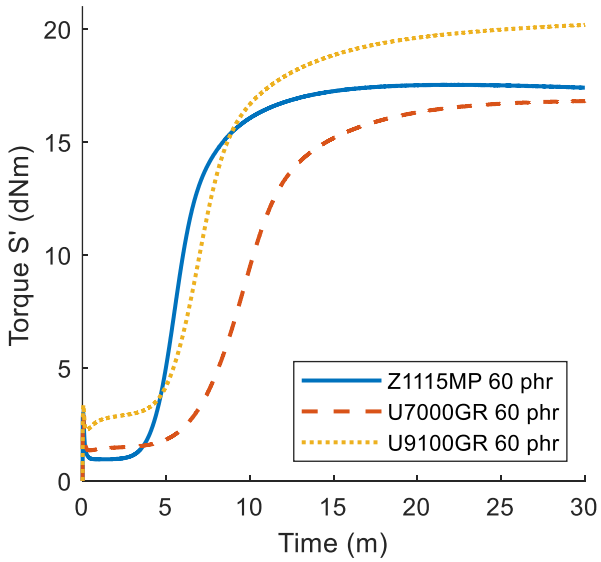

Figure 43: Cure curves of SBR 4601 / BR Cis-132 compounds using 60 phr of various silica types.

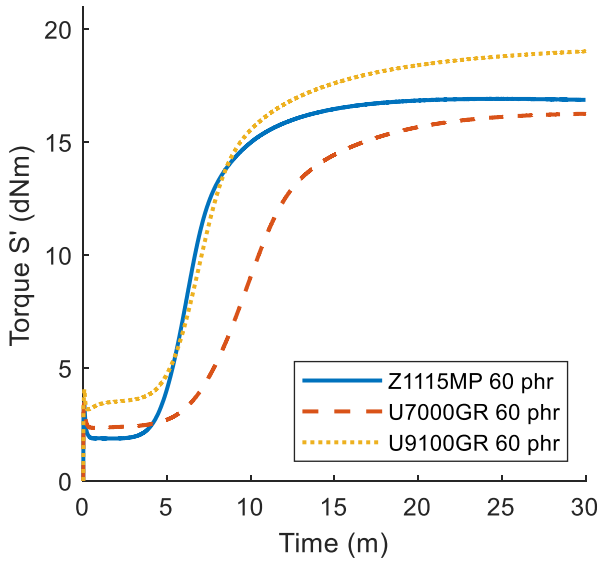

Figure 44: Cure curves of SBR 4602 / BR Cis-132 compounds using 60 phr of various silica types.

4.4.3 Mechanical behavior

Hardness

Hardness results of compounds using varying types of silica are shown in Figure 45. Hardness increases with increasing silica SSA, with the largest increase seen between silica U7000GR and silica U9100GR.

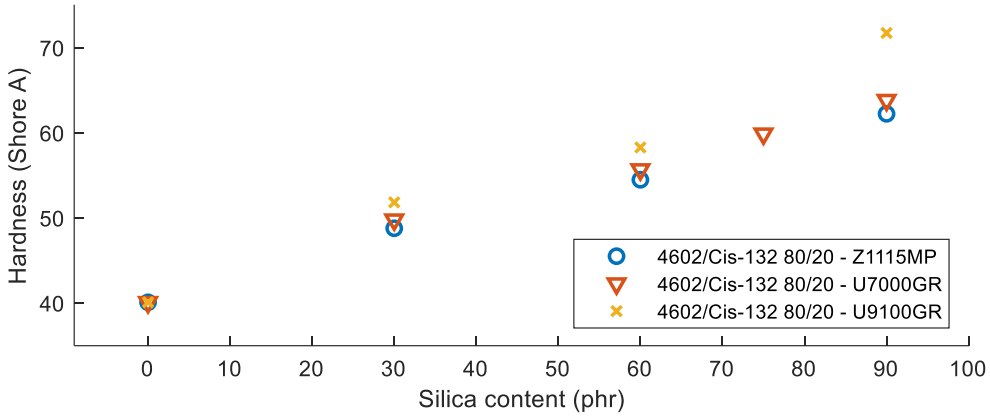

Figure 45: Hardness values of 4602/Cis-132 compounds with varying silica types.

Stress-strain behavior

The mechanical properties of SBR/BR compounds with varying silica types are shown in Table 17. Somewhat counterintuitively, no correlation between silica surface area and mechanical properties can be seen. Compounds using silica U9100GR show both the lowest reinforcement index, but highest stress and elongation at break.

Table 17: Mechanical properties of SBR/BR compounds using varying silica types, with 90 phr silica content.

Polymers	Blend	Silica	$M_{100\%}$ (MPa)	$M_{300\%}$ (MPa)	M_{300}/M_{100}	σ_b (MPa)	ε_b (%)
4601/Cis-132	80/20	Z1115MP	3,4	12,5	3,7	14,4	342
4602/Cis-132	80/20	Z1115MP	3,1	15,8	5,2	17,0	323
4601/Cis-132	80/20	U7000GR	3,1	13,1	4,2	14,5	325
4602/Cis-132	80/20	U7000GR	2,8	14,0	5,1	12,9	280
4601/Cis-132	80/20	U9100GR	3,2	11,1	3,5	16,5	406
4602/Cis-132	80/20	U9100GR	3,6	13,0	3,6	18,2	387

The similar performance between different silica types can be explained by the difference in curing behavior of the different silica types. It is theorized that compounds using silica Z1115MP reach a higher crosslink density (CLD), as less of the accelerators is absorbed by the lower amount of silica surface area. The opposite is achieved with silica U9100GR, which absorbs more accelerators and therefore reaches a lower CLD. This results in either low reinforced compounds with a high CLD or high reinforced compounds with low CLD, resulting in similar mechanical properties as can also be seen in Figure 46 and Figure 47.

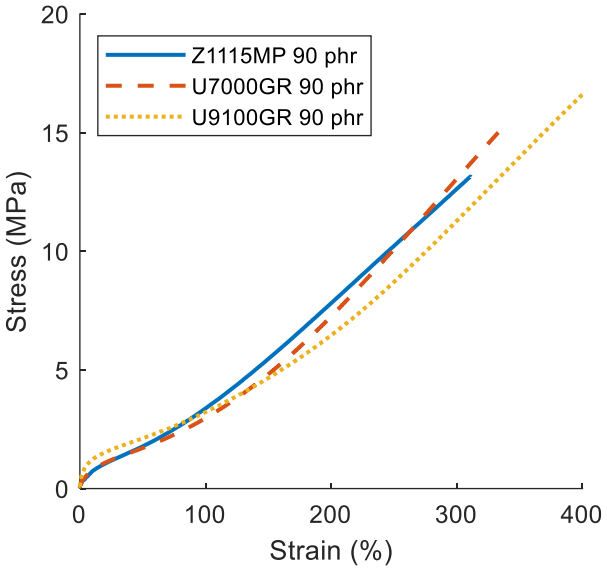

Figure 46: Stress-strain curves of SBR 4601 / BR Cis-132 compounds with varying silica types, using 90 phr of silica.

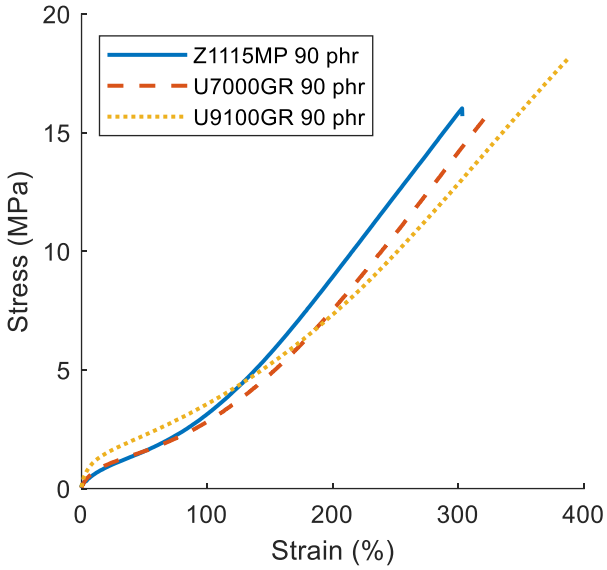

Figure 47: Stress-strain curves of SBR 4602 / BR Cis-132 compounds with varying silica types, using 90 phr of silica.

4.4.4 Dynamic behavior

Rebound

Figure 48 shows the room temperature rebound resilience of SBR 4602 / BR Cis-132 compounds with varying silica types. Especially at high silica loadings, an increase in rebound is seen when reducing the SSA of the silica. This can be attributed to an expected better dispersion and decrease in filler-filler interaction with low SSA silica, which decreases the energy losses due to hysteresis.

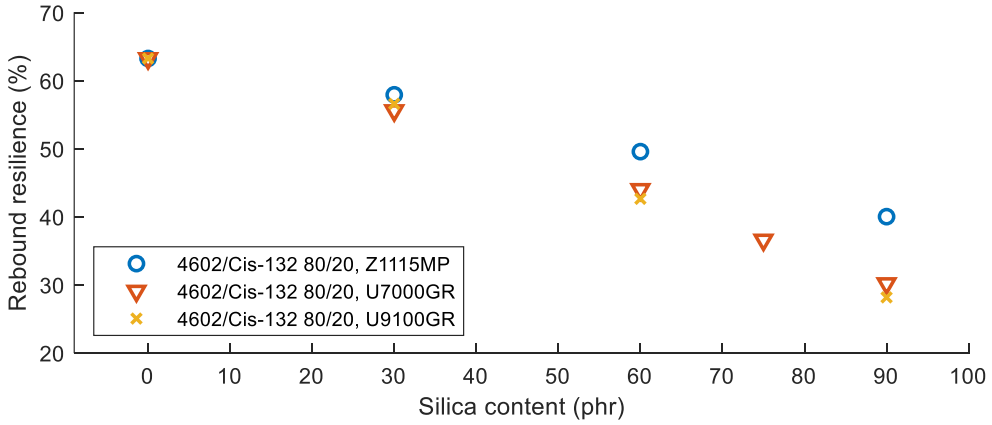

Figure 48: Room temperature rebound resilience of SBR 4602 / BR Cis-132 compounds with varying silica types.

Dynamic Mechanical Analysis

Figure 49 shows the loss angle curves of SBR 4602 / BR Cis-132 compounds using varying silica types. Around T_g, the compound using silica U9100GR shows a lower tan(δ) value compare to the lower SSA silicas, with the tan(δ) decreasing with increasing silica SSA. With an increase in SSA, the amount of bound rubber increases. Bound rubber can be described as a shell of polymer around filler particles that have reduced mobility [30]. This immobilized layer is very elastic in nature. Since a higher amount of bound rubber occurs in compounds using high SSA silica, the elasticity is relatively high around the Tg. This results in a lower tan(δ) value around T_g compared to compounds using lower SSA silica. These effects still visible around 0 °C, meaning silica Z1115MP shows the best indicator for wet grip, with the tan(δ) value decreasing with increasing silica SSA.

With increasing temperature, the immobilized polymer shell decreases, meaning internal friction of the filler starts to have a larger impact on the tan(δ) value. With the lowest SSA, silica Z1115MP has the least filler-filler interaction, resulting in a lower tan(δ) value at both room temperature and 60 °C, with tan(δ) increasing with increasing silica SSA. This supports the findings for rebound in the previous section. Additionally, the rolling resistance indicator tan(δ) at 60 °C shows a reduced rolling resistance for the compound using silica Z1115MP.

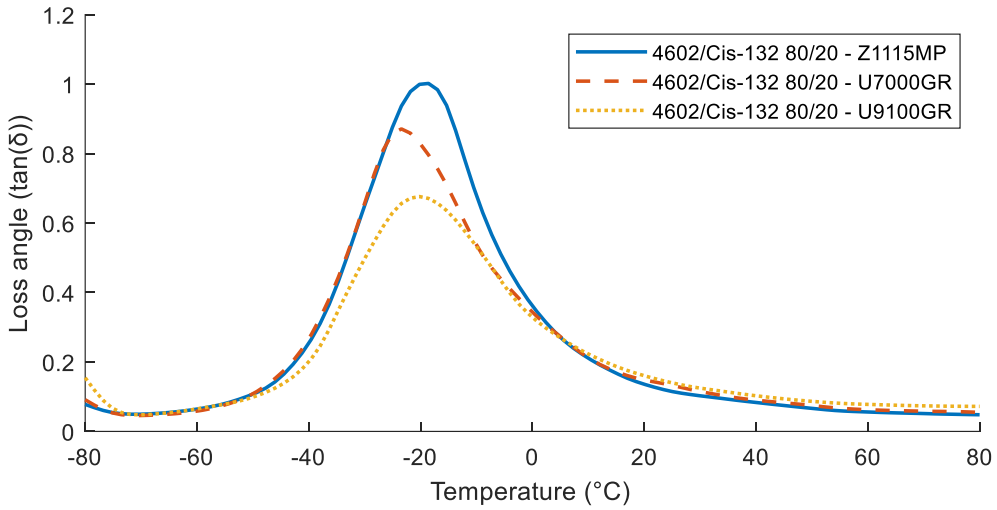

Figure 49: DMA curve of SBR 4602 / BR Cis-132 compounds with 60 phr silica of varying types.

CHAPTER 5
CONCLUSIONS

In this study, different combinations of elastomer types, silica content and silica types were compounded using a tire tread formulation. The effects of these combinations on processability, vulcanization behavior, mechanical properties and dynamic properties were studied. As a result, more insight was gained in the usage of functionalized elastomers, elastomer blends, silica types, and silica loading in a green tire tread compound.

5.1 Research summary

Several aspects of tire production and tire performance were examined. The following conclusions can be made.

5.1.1 Processability

The usage of silica functionalized elastomers negatively impacts the processability of a tire tread compound, as its viscosity increases significantly due to an interaction between the functional group and the silica filler before functionalization. This increase in viscosity can be negated somewhat by using an SBR/BR blend, which lowers the viscosity, allowing for acceptable processability at higher silica loadings. The addition of high specific surface area silica to a compound using silica functionalized elastomers is not recommended, as both the high specific surface area as well as the functionalization have a large impact on the viscosity increase of the compound, making it very difficult to process. On the other hand, low surface area silica decreases the viscosity, allowing for higher silica contents to still have acceptable processability.

5.1.2 Vulcanization behavior

Vulcanization behavior is only slightly influenced by the usage of silica functionalized elastomers, as an interaction is suspected between the functionalized group and the curatives used in the compound. The change of silica content and specific surface area affect the vulcanization behavior significantly, with possibly the cure torque above the percolation threshold being dictated mainly by the filler-filler interaction. Additionally, the change in silica specific surface area likely affects the crosslink densities of the cured compounds.

5.1.3 Mechanical behavior

Mechanical properties are not significantly affected by the use of silica functionalized elastomer, but are degraded when the fraction of BR in the compound is increased. Changing the silica specific surface area produced similar results, as the crosslink densities of the compounds were suspected to be different.

5.1.4 Dynamic behavior

The usage of silica functionalized SBR in a green tire tread compound results in slightly improved wet grip and rolling resistance indicators compared to compounds using non silica functionalized SBR. The addition of BR has a slight negative impact on the rolling

resistance indicator and decreases the wet grip indicator significantly. Rolling resistance and wet grip indicators both improve with decreasing silica surface area, but will likely decrease the wear resistance of the compound.

5.2 Recommendations

Some aspects of the research performed in this thesis can be improved upon in the future. The following points of improvement can be made:

5.2.1 Processability

Payne effect measurements using the RPA are implemented for several investigations, including micro-dispersion of the filler. In the case of comparing dispersion quality between functionalized and non-functionalized elastomers, using the Payne effect is not suitable, as increased filler-polymer interaction between the functionalized rubber and the filler increases the measured Payne effect. Additionally, the variation of silica specific surface area also presented some unexpected results that do not allow for comparisons between silica types. This means that optical microscopy or a dispergrader should be used to have more definitive conclusions on dispersion improvement.

Additionally, the strain range of the Payne effect measurements could be extended, as the lower plateau is not fully reached at 100% strain. This could be done to give more insight into the filler-polymer interactions that possibly occur in the functionalized polymer before vulcanization.

In addition to high strain Payne effect measurements, further investigations of bound rubber content could be performed to better indicate the filler-polymer structure in the uncured compounds.

5.2.2 Vulcanization behavior

During vulcanization of the compounds, some results were unexpected. The influence of silica content and surface area on the cure characteristics could hypothetically be explained by the filler-filler interaction above the percolation threshold having a large influence on the cure torque, but no definitive conclusions could be made. Therefore, this effect could be investigated further in future studies.

5.2.3 Mechanical behavior

Due to large deviations between samples, data for stress and strain at break of the tensile samples was difficult to interpret. This could be improved by increasing the sample size of the tested compounds.

Additionally, an investigation on crosslink density could be performed to give an explanation why the tensile properties of compounds using different silica specific surface area are similar.

5.2.4 Dynamic behavior

Some results from DMA tests had to be disregarded, as their outcomes were unlikely to be accurate. It remains unclear if this was due to material inconsistencies or faulty measurement equipment. Some experiments should be repeated in the future to gain the proper results or to determine the origin of these deviations.

REFERENCES

[1] "CO2 emissions from cars: facts and figures," *European Parliament*, Mar. 22, 2019. https://www.europarl.europa.eu/news/en/headlines/society/20190313STO31218/co2-emissions-from-cars-facts-and-figures-infographics (accessed May 01, 2023).

[2] "'Fit for 55': Council adopts regulation on CO2 emissions for new cars and vans - Consilium," *European Council*, 2023. https://www.consilium.europa.eu/en/press/press-releases/2023/03/28/fit-for-55-council-adopts-regulation-on-co2-emissions-for-new-cars-and-vans/ (accessed May 01, 2023).

[3] N. Ireson, "How Tires Can Affect Your EV's Range and Performance," *Motor Trend*, 2022. https://www.motortrend.com/features/ev-tire-range-performance/ (accessed May 01, 2023).

[4] "The Green Tire," *Evonik Industries AG*. https://corporate.evonik.com/en/the-green-tire-1456.html (accessed Apr. 14, 2023).

[5] S. Thiele, J. Kiesekamp, S. Rulhoff, and D. Bellgardt, "Modified Synthetic Rubber for Silica & Carbon Black Containing Tire Treads," *KGK Rubberpoint*, vol. 64, pp. 36–41, Nov. 2011, [Online]. Available: www.kgk-rubberpoint.de

[6] A. N. Gent, "Rubber - Development of the natural rubber industry," *Encyclopædia Britannica*. https://www.britannica.com/science/rubber-chemical-compound/Development-of-the-natural-rubber-industry (accessed Nov. 20, 2022).

[7] C. McFadden, "Charles Goodyear: Inventions, Experiments and Biography," *Interesting Engineering*, Dec. 17, 2017. https://interestingengineering.com/culture/charles-goodyear-the-father-of-vulcanization (accessed Nov. 25, 2023).

[8] Z. Frank and A. Mustacchio, "The International Natural Rubber Market, 1870-1930," *Economic History Association*, Mar. 16, 2008. https://eh.net/encyclopedia/the-international-natural-rubber-market-1870-1930/ (accessed Apr. 29, 2023).

[9] "The natural rubber production in the World," *Knoema*. https://knoema.com/data/agriculture-indicators-production+natural-rubber (accessed Apr. 29, 2023).

[10] "U.S. Synthetic Rubber Program ," *American Chemical Society*, Aug. 29, 1998. https://www.acs.org/education/whatischemistry/landmarks/syntheticrubber.html (accessed Apr. 29, 2023).

[11] B. Rodgers, *Rubber compounding: chemistry and applications*, 2nd ed. CRC Press, 2016.

[12] A. Blume and S. Saiwari, "Elastomer Science & Engineering - Natural Rubber and Isoprene Rubber." University of Twente, 2022.

[13] "Isoprene Rubber," *Crow Polymer Database*. https://polymerdatabase.com/Polymer%20Brands/Isoprene.html (accessed May 10, 2023).

[14] “Butadiene Rubber,” *Crow Polymer Database*. https://www.polymerdatabase.com/Elastomers/BR.html (accessed May 10, 2023).

[15] A. Blume, “Elastomer Science & Engineering - Butadiene Rubber and Styrene Butadiene Rubber.” University of Twente, 2022.

[16] “Styrene-Butadiene Rubber,” *Crow Polymer Database*. https://www.polymerdatabase.com/Elastomers/SBR.html (accessed May 10, 2023).

[17] “Styrene-butadiene,” *Wikipedia*. https://en.wikipedia.org/wiki/Styrene-butadiene (accessed May 11, 2023).

[18] C. Yamada, “Influence of functionalized S-SBR on silica-filled rubber compound properties,” University of Twente, Enschede, 2023.

[19] R. J. Dhanorkar, S. Mohanty, and V. K. Gupta, “Synthesis of Functionalized Styrene Butadiene Rubber and Its Applications in SBR-Silica Composites for High Performance Tire Applications,” *Industrial and Engineering Chemistry Research*, vol. 60, no. 12. American Chemical Society, pp. 4517–4535, Mar. 31, 2021. doi: 10.1021/acs.iecr.1c00013.

[20] S. Maghami, “Silica-filled tire tread compounds: an investigation into the viscoelastic properties of the rubber compounds and their relation to tire performance,” University of Twente, Enschede, The Netherlands, 2016. doi: 10.3990/1.9789036541282.

[21] A. Mazumder, J. Chanda, S. Bhattacharyya, S. Dasgupta, R. Mukhopadhyay, and A. K. Bhowmick, “Improved tire tread compounds using functionalized styrene butadiene rubber-silica filler/hybrid filler systems,” *J Appl Polym Sci*, vol. 138, no. 42, Sep. 2021, doi: 10.1002/app.51236.

[22] J. L. Tardiff, M. Harper, D. Haakenson, M. Joandrea, and M. Knych, “Effect of sSBR composition, functionality on tire tread compound performance,” *Rubber and Tire Digest*, vol. 3, no. 5, pp. 23–34, Aug. 2018.

[23] F. Grunert and A. Blume, “Elastomer Science & Engineering - Reinforcement.” University of Twente, 2022.

[24] J. E. Mark, B. Erman, and M. Roland, *The Science and Technology of Rubber*, 4th ed. Academic Press, 2013.

[25] “How is Carbon Black Produced?,” *International Carbon Black Association*. https://www.carbon-black.org/is-carbon-black-safe (accessed May 30, 2023).

[26] F. Grunert, “Elastomer Science & Engineering - Carbon Black Morphology and Characterization.” University of Twente, 2022.

[27] D. Maschke and A. Blume, “Elastomer Science & Engineering - Silica Production and Characterization.” University of Twente, 2021.

[28] A. Blume, J. Jin, A. Mahtabani, X. He, S. Kim, and Z. Andrzejewska, “New Structure Proposal for Silane Modified Silica,” 2019.

[29] A. Blume, “Elastomer Science & Engineering - Silica Silane Coupling.” University of Twente, 2022. [Online]. Available: https://www.google.de/search?q=coffee+break&source=lnms&tbm=isch&biw=1920&bih=1041#imgrc=Yepabf19YHanjM

[30] M.-J. Wang, “Effect of Polymer-Filler and Filler-Filler Interactions on Dynamic Properties of Filled Vulcanizates,” *Rubber Chemistry and Technology*, vol. 71, no. 3, pp. 520–589, Jul. 1998, doi: 10.5254/1.3538492.

[31] A. Franck, “Viscoelasticity and dynamic mechanical testing A. Franck, TA Instruments Germany.”

[32] A. Blume, “Elastomer Science & Engineering - Introduction.” University of Twente, 2022.

[33] “Frequency Dependence of Glass Transition Temperatures.” [Online]. Available: www.tainstruments.com/

[34] B. Taillet, “New possibilities for characterizing elastomers using Dynamic Mechanical Analysis (DMA) at high strain rates.” Mar. 13, 2020.

[35] “Tyres - Energy labelling requirements.” https://commission.europa.eu/energy-climate-change-environment/standards-tools-and-labels/products-labelling-rules-and-requirements/energy-label-and-ecodesign/energy-efficient-products/tyres_en (accessed May 14, 2023).

[36] S. Ling, F. Yu, D. Sun, G. Sun, and L. Xu, “A comprehensive review of tire-pavement noise: Generation mechanism, measurement methods, and quiet asphalt pavement,” *J Clean Prod*, vol. 287, Mar. 2021, doi: 10.1016/j.jclepro.2020.125056.

[37] U. Sandberg, “Tyre/road noise - Myths and realities,” in *The 2001 International Congress and Exhibition on Noise Control Engineering*, The Hague, Aug. 2001.

[38] J. Winroth, C. Hoever, W. Kropp, and T. Beckenbauer, “The contribution of air-pumping to tyre/road noise,” in *Proceedings of AIA-DAGA 2013*, 2013, pp. 1594–1597.

[39] “Sprintan SLR 4601-Schkopau.” Trinseo, 2020.

[40] “Sprintan SLR 4602-Schkopau.” Trinseo, 2020.

[41] “Buna Cis-132 - Schkopau.” Songhan Plastic Technology.

[42] “Buna CB-24 - Dormagen.” Arlanxeo, 2008.

[43] F. Grunert, “Analytical method development to predict the in-rubber dispersibility of silica,” University of Twente, Enschede, 2018.

[44] “Ultrasil 9100 GR.” Evonik Industries AG, 2021.

[45] “Ultrasil 7000 GR.” Evonik Industries AG, 2012.

[46] “Solvay silica ranges for tires: the world class reference for energy efficient tires.” Solvay Silica. [Online]. Available: www.solvay.com

[47] L. Guy, S. Daudey, P. Cochet, and Y. Bomal, “New Insights in the Dynamic Properties of Precipitated Silica Filled Rubber Using a New High Surface Silica,” *KGK Rubberpoint*, vol. 62, no. 7–8, pp. 383–391, 2009.

[48] J. Jin, J. W. M. Noordermeer, W. K. Dierkes, and A. Blume, “The effect of silanization temperature and time on the marching modulus of silica-filled tire tread compounds,” *Polymers (Basel)*, vol. 12, no. 1, Jan. 2020, doi: 10.3390/polym12010209.

[49] C. Hayichelaeh, L. A. E. M. Reuvekamp, W. K. Dierkes, A. Blume, J. W. M. Noordermeer, and K. Sahakaro, “Reinforcement of natural rubber by silica/silane in dependence of different amine types,” *Rubber Chemistry and Technology*, vol. 90, no. 4, pp. 651–666, Dec. 2017, doi: 10.5254/rct.82.83708.

[50] “ISO 289 - Rubber, unvulcanized - Determinations using a shearing-disc viscometer,” Geneva, 2003.

[51] S. Mihara, R. N. Datta, and J. W. M. Noordermeer, “Flocculation in silica reinforced rubber compounds,” *Rubber Chemistry and Technology*, vol. 82, no. 5, pp. 524–540, Nov. 2009.

[52] “ISO 6502 - Rubber - Guide to the use of curemeters,” Geneva, 1999.

[53] “ASTM D2240 - Standard Test Method for Rubber Property - Durometer Hardness,” West Conshohocken, 2002.

[54] “ISO 37 - Rubber, vulcanized or thermoplastic - Determination of tensile stress-strain properties,” Geneva, 2012.

[55] “ISO 4662 - Rubber, vulcanized or thermoplastic-Determination of rebound resilience,” Geneva, 2009.

[56] “ISO 4664-1 - Rubber, vulcanized or thermoplastic - Determination of dynamic properties - Part 1,” Geneva, 2011.

[57] J. Jin, J. W. M. Noordermeer, A. Blume, and W. K. Dierkes, “Effect of SBR/BR elastomer blend ratio on filler and vulcanization characteristics of silica filled tire tread compounds,” *Polym Test*, vol. 99, Jul. 2021, doi: 10.1016/j.polymertesting.2021.107212.

BIOGRAPHY

Simon Rezelman is a student who started his bachelor's degree in Mechanical Engineering in 2016 at the University of Twente. After graduating in 2020, he continued with the Master's degree in Mechanical Engineering, specializing in High-Tech Systems and Materials.

UNIVERSITY OF TWENTE

Drienerlolaan 5

7522 NB Enschede

P.O.Box 217

7500 AE Enschede

P +31 (0)53 489 9111

info@utwente.nl

www.utwente.nl